This is a preprint, the final version is subject to change, of the American Mineralogist (MSA)
Cite as Authors (Year) Title. American Mineralogist, in press.
(DOI will not work until issue is live.) DOI: http://dx.doi.org/10.2138/am-2015-4967

Pre-Eruptive Magma Mixing and Crystal Transfer Revealed by Phenocryst and Microlite Compositions in Basaltic Andesite from the 2008 Eruption of Kasatochi Island Volcano – REVISION #2

Owen K. Neill[1a], Jessica F. Larsen[2], Pavel E. Izbekov[2], Christopher J. Nye[3]

[1]Peter M. Hooper GeoAnalytical Laboratory, School of the Environment, Washington State University, P.O. Box 642812, Pullman, WA 99164-2812
owen.neill@wsu.edu
[a]Corresponding author.

[2]Geophysical Institute, University of Alaska Fairbanks, 903 Koyukuk Drive, Fairbanks, AK 99775
jflarsen@alaska.edu, pavel@gi.alaska.edu

[3]Alaska Volcano Observatory, State of Alaska, Division of Geological and Geophysical Surveys, 3354 College Road, Fairbanks, AK 99709
cnye2@gi.alaska.edu

ABSTRACT

The 7-8 August, 2008 eruption of Kasatochi Island volcano, located in the central Aleutians Islands, Alaska, produced abundant, compositionally heterogeneous basaltic andesite (52-55 wt% SiO_2) that has been interpreted to result from pre-eruptive magma mixing. The basaltic andesite contains two populations of plagioclase phenocrysts. The first, volumetrically dominant population consists of oscillatory-zoned phenocrysts with an overall normal zonation trend towards comparatively sodic rims (An_{55-65}), interrupted by dissolution features and spikes in calcium content (up to ~An_{85}). The second population consists of phenocrysts with highly calcic compositions (~An_{90}). These phenocrysts contain sharp decreases in calcium content close to their rims (reaching as

low as ~An_{60}), but are otherwise texturally and compositionally homogeneous. Groundmass plagioclase microlites are generally much more calcic than rims of the first phenocryst population, with more than 50% of measured microlites containing >An_{80}. Major, minor and trace element concentrations of plagioclase microlites and phenocrysts indicate that oscillatory-zoned phenocrysts derived from cooler (800-950 °C), more silicic mixing magma, while unzoned, calcic phenocrysts were associated with hotter (900-1050 °C), mafic magma. The mixing of these magmas just prior to eruption, followed by decompression during the eruption itself created high effective undercoolings in the mafic end member, and lead to the nucleation of high-An microlites. MgO and FeO concentrations of plagioclase microlites and high-An phenocryst rims (up to ~0.4 and ~1.3 wt%, respectively) provide further evidence for high mixing- and eruption-induced effective undercoolings.

Keywords: Kasatochi; Aleutian volcanism; magma mixing; plagioclase; microlites.

INTRODUCTION

Plagioclase microlites in volcanic systems

Plagioclase microlites are small (<100 μm) crystals of plagioclase feldspar, which are generally assumed to crystallize in response to degassing and decompression, both of which will cause high effective undercoolings during the final ascent of magma from shallow crustal storage regions to the surface (e.g. Westrich et al. 1988; Geschwind and

Rutherford 1995; Hammer and Rutherford 2002; Martel and Schmidt 2003; McCanta et al. 2007; Brugger and Hammer 2010). For the purposes of this study, the term microlite will refer to crystals <100 μm in length, while the term "phenocryst" will refer to crystals within the sample >300 μm in length. Crystallization during magmatic ascent is the last phase of crystallization before an erupted magma freezes. If all microlites are assumed to grow during ascent, their abundance and texture may reflect the ascent rate of the magma from depth (e.g. Hammer and Rutherford 2002; Martel 2012). Also, microlites forming during ascent are typically assumed to grow from the most evolved, relatively low-Ca, high-Na, high-K liquids within the system, and therefore microlite compositions would be compositionally similar, or even higher in Na and K than the rim compositions of plagioclase phenocrysts (e.g. Blundy and Cashman 2001).

There are, however, systems that do not conform to this general model, containing microlites that are more anorthitic than the dominant phenocryst rim compositions. In these cases, microlites may have been inherited from a pre-eruptive mixing end member. For example, Martel et al. (2006) reported microlites with compositions up to ~An_{90}, well in excess of phenocryst rim compositions (An_{50-60}), in a study of Mount Pelée, Martinique. Mount Pelée, like Kasatochi, had produced andesite and basaltic andesite in the same eruptive sequence, and Martel et al. (2006) inferred that the highly calcic microlites were inherited from basaltic replenishment of the magmatic system immediately prior to eruption. In a study of Soufriere Hills Volcano, Montserrat, Couch et al. (2003) suggested that high-An microlites crystallized in a compositionally-zoned magma storage region, whereby hotter, more calcic liquid ascended rapidly within the magma chamber due to thermally-driven convection, causing the crystallization of high-

An microlites, which were then mixed with cooler, more evolved andesite at the top of the system. Further study of the Soufriere Hills by Humphreys et al. (2009; 2010) revealed that mafic magmatic inclusions incorporated in the deeper region of the magmatic system may also contain plagioclase microlites, which are then transferred to silicic magma in the upper reaches of the magmatic system when the inclusions disaggregate.

Basaltic andesite clasts from the 2008 eruption of Kasatochi also contain a population of plagioclase microlites that are more calcic than the rims of the dominant phenocryst population. In this paper, the plagioclase phenocryst and microlite populations, as well as the amphibole and titanomagnetite phenocryst populations of the 2008 Kasatochi basaltic andesite are characterized to investigate the origins and conditions of formation of the individual populations. The goal of this study is to decipher whether the high-An microlites seen in the 2008 Kasatochi basaltic andesite were derived from basaltic replenishment, similar to a model for formation of similar microlites at Mount Pelée. Major and minor element compositions of plagioclase phenocrysts and microlites from the basaltic andesite, in addition to bulk-rock and mafic mineral compositions, indicate that the microlites are indeed the product of pre-eruptive mixing, involving crystal transfer between two compositionally and thermally different mixing end members.

Geologic setting

Kasatochi Island, located in the Central Aleutian Islands (Figure 1), is a 3-km wide stratovolcano, rising ~300 m above sea level. The edifice consists of a single composite volcanic cone with a central crater ~1 km wide. The central crater also contains a brackish lake. Deposits from eruptions prior to 2008 consist of a basal unit of interlayered lahars, lava flows, pyroclastic deposits and hyaloclastites; a middle series of lava flows ranging in composition from basalt to andesite; and an uppermost interlayered pyroclastic surge/flow unit (Waythomas et al. 2010a). Due to the island's remote location, and the lack of historical eruptions, no geologic studies targeting Kasatochi existed prior to 2008, though studies of the island's flora and fauna had been ongoing since the 1980's (Williams et al. 2010, and references therein). Geologic studies of the island were limited to preliminary surveys and mapping of the area (e.g. Coats 1956), and chemical analyses of one basaltic sample, originally reported in Kay and Kay (1985) and used in subsequent studies of arc petrogenesis in the Aleutians (e.g. Yogodzinski et al. 1995; Yogodzinski and Kelemen 1998).

Anomalously strong seismic activity was detected at Kasatochi on 6 August, 2008, and on 7 August, the first ash plume was detected, marking the onset of explosive activity. The eruption continued for ~21 hours after the first ash plume, punctuated by 5 main explosive events (Arnoult et al. 2010; Fee et al. 2010). Waythomas et al. (2010a, 2010b) and Scott et al. (2010) describe the eruption sequence in detail. To summarize, the eruption produced ash plumes which reached up to 18 km above sea level, released more seismic energy than any volcanic eruption ever recorded by the Alaska Volcano Observatory, the agency responsible for monitoring Aleutian volcanoes, and was the single largest point-source release of SO_2 gas since the 1991 eruptions of Cerro Hudson

in Chile and Pinatubo in the Philippines. In addition, the eruption produced voluminous pyroclastic flows and surges, leaving tephra deposits up to 30 m thick, which increased the diameter of the island by ~800 m.

A representative suite of juvenile pyroclasts and gabbro blocks was collected from the 2008 Kasatochi deposits during trips to the island in the summers of 2008, 2009, 2010 and 2011. Full descriptions and interpretations of the petrography and geochemistry of the 2008 Kasatochi eruptive products are available in Neill (2013). This study includes relevant subsets of the data from those studies, as well as new characterizations of the basaltic andesite plagioclase populations that shed further light on pre-eruptive mixing and crystal transfer within the basaltic andesite.

ANALYTICAL METHODS

Compositions of amphibole, titanomagnetite and groundmass glass were analyzed by wavelength-dispersive x-ray spectrometry using the 4-spectrometer CAMECA SX-50 electron microprobe, housed at the Advanced Instrumentation Laboratory of the University of Alaska Fairbanks. Concentrations were obtained from raw counts using a ZAF intensity correction. Amphibole and titanomagnetite analyses were conducted with a focused beam, while groundmass glass analyses were conducted with the beam defocused to a radius of ~10 μm to minimize Na, K, Al and Si migration during analyses (cf. Morgan and London 1996). Na loss was corrected using a variation of the procedures of Nielsen and Sigurdsson (1981) via ProbeForEPMA software (Donovan et al. 2007).

Plagioclase phenocryst and microlite compositions microlites were analyzed by electron microprobe using two separate analytical procedures. A routine optimized for speed and accurate determination of anorthite content was used for an initial survey of plagioclase phenocryst cores and rims (hereafter referred to as the "R1" routine). A second set of phenocrysts, and all plagioclase microlites, were then analyzed using higher currents and longer counting times, in order to obtain more accurate analyses of the minor elements Fe and Mg (reported as oxides FeO and MgO, with all Fe reported as Fe^{2+}). In the second routine (referred to as the "R2" routine), the electron beam was defocused to ~3 μm and Na peak counting time was reduced to 10 seconds to minimize Na migration; no significant migration of Na, K or Al was detected during analyses under either R1 or R2 conditions. Typical detection limits for FeO and MgO, calculated using ProbeForEPMA software as described in Donovan et al. (2007), were 0.02 and 0.005 wt%, respectively. Microprobe analyses of microlites were performed as close to the rims of the microlites as possible.

Analytical conditions, calibration standards and typical analytical uncertainties for all electron microprobe analyses may be found in Appendix 1. Individual EPMA analyses are compiled in Appendices 2-9.

RESULTS

Petrography and bulk chemistry of 2008 Kasatochi samples

The 2008 Kasatochi eruption produced two main juvenile lithologies; a white, pumiceous, medium-K, borderline calk-alkaline andesite, ranging from ~58-62 wt% SiO_2

(Figure 2); and a denser, grey-brown, medium-K, tholeiitic basaltic andesite, ranging from ~52-55 wt% SiO_2 (Figure 2). Banded clasts, representing mechanical mixtures between the andesite and basaltic andesite, are also common throughout the 2008 pyroclastic deposits. All juvenile products of the 2008 eruption contain a phenocryst assemblage of plagioclase, clinopyroxene, orthopyroxene, amphibole and titanomagnetite. Andesite compositions do not vary systematically in all components; while andesite large-ion lithophile and high field strength element concentrations form linear arrays in most element vs. SiO_2 diagrams, other components, such as the heavy rare-earth elements and P_2O_5, show little systematic variations (Figure 2). However, basaltic andesite samples lie along approximately linear arrays in element-element diagrams (Figure 2), and the trends do not intersect the andesite concentrations for many components (e.g. Al_2O_3, P_2O_5, Y, Yb, Zn; Figure 2).

Plagioclase phenocryst compositions

There are two distinct populations of plagioclase phenocrysts in the basaltic andesite. The first population (referred to herein as Group 1 phenocrysts) consists of oscillatory-zoned plagioclase phenocrysts, with an overall normal zonation trend sometimes interrupted by spikes in An content (Figure 3). Group 1 core compositions vary from ~An_{55-90}, with some phenocrysts containing homogeneous or sieved high-An cores (Figure 3, 4). The rims of Group 1 phenocrysts, however, are more homogeneous, as ~70% of Group 1 phenocrysts have rim compositions between An_{55-65} (Figure 4).

The second major phenocryst population (Group 2) consists of highly calcic (>An_{80}; Figure 4, 5), texturally homogeneous plagioclase phenocrysts with no dissolution features beyond scattered small (<10 μm) melt inclusions. Group 2 phenocrysts account for ~30% of the overall basaltic andesite plagioclase phenocryst population. Compared to Group 1 phenocrysts, Group 2 phenocrysts contain very few compositional variations within individual crystals. Some crystals have cores with >An_{90}, which is higher than the dominant composition, though the boundaries of these zones are not marked by any observable textural features (Figure 5). Also, as can be seen in both compositional profiles (Figure 5) and backscatter-electron imagery (Figure 5, 6) of Group 2 phenocrysts, the outermost 20-30 μm of some Group 2 phenocrysts frequently show sharp decreases in An content.

Plagioclase microlite compositions

Plagioclase microlite compositions vary across a wide range of An contents (An_{55-95}, Figure 4), but the modal composition (~An_{85}) is approximately 25 mol% higher than the modal rim composition (~An_{60}) of the volumetrically dominant Group 1 phenocryst population. Only ~10% of microlites have An contents equivalent to the compositional mode of the Group 1 rims (An_{55-65}, Figure 4), while ~50% of microlites have An contents >An_{80}. Larger microlites show some degree of zonation, with lower-An rims (An_{57-79}) surrounding higher-An cores (An_{80-87}; Figure 6). Measurements of microlite compositions were made as close to rims as possible, and therefore generally high-An microlite

compositions indicate that either most microlites are unrimmed, or that the rims are generally smaller than can be analyzed quantitatively.

Plagioclase FeO and MgO concentrations

Variations in the major element concentrations of plagioclase do not always point to a unique cause, since the An-Ab exchange reaction in plagioclase is a function of multiple processes (T, X, p_{H2O}; reviewed in depth by Lange et al. 2009). Coupling examinations of major elements in plagioclase with variations in the concentrations of minor and trace elements, such as iron and magnesium, may help link such compositional fluctuations to specific magmatic processes (e.g. Phinney 1992; Singer et al. 1995; Ginibre et al. 2002; Humphreys et al. 2006). Group 1 plagioclase core and rim FeO and MgO contents are approximately equivalent, even in crystals with high-An cores (Figure 3, 7), and the spikes in An content common in Group 1 phenocrysts are also not correlated with any significant change in FeO or MgO (Figure 3). Iron and magnesium contents of Group 1 plagioclase phenocrysts generally do not vary within individual grains by more than analytical uncertainty, though the transition from high-An cores to oscillatory rims in some Group 1 phenocrysts is sometimes correlated with an increase in MgO (Figure 3). While analytical uncertainties associated with both FeO and MgO measurements are relatively large, both the cores and rims of Group 1 phenocrysts contain between 0.4 and 0.65 wt% FeO, while MgO concentrations of Group 1 phenocryst cores and rims are generally near 0.05 wt% (Figure 7).

FeO and MgO contents of Group 2 phenocryst cores generally match those of Group 1, containing between ~0.4 and ~0.65 wt% FeO and MgO concentrations ~0.05 wt% (Figure 7). Within the homogenous, high-An zones in the interiors of Group 2 phenocrysts, systematic changes in FeO and MgO contents within individual grains are generally lacking (Figure 5). However, the Group 2 phenocrysts that display abruptly decreasing An content in their outermost few tens of microns also contain corresponding spikes in both FeO and MgO, reaching up to 1.3 wt% FeO and 0.4 wt% MgO (Figure 5, 7). Concentrations of FeO and MgO in microlites are highly variable. Only ~20% of measured microlites contain FeO <0.65 wt%, similar to Group 1 phenocrysts, with the maximum microlite FeO concentration reaching ~1.3 wt%. There is also a generally negative correlation between anorthite content and both MgO and FeO concentration in both microlites and Group 2 phenocryst rims, although more sodic microlites with low-Fe and low-Mg contents do exist (Figure 7).

Compositions of groundmass glass and mafic minerals

Groundmass glass compositions in the basaltic andesite are heterogeneous, varying from ~60-70 wt% SiO_2, ~13-17 wt% Al_2O_3, and ~1.2-2.6 wt% K_2O (Figure 8). MgO concentrations reach a maximum of 3 wt%, while FeO concentrations are between ~2.5 and ~8 wt%. Groundmass glass compositions qualitatively mirror trends in bulk-rock compositions, varying along scattered linear trends, with both MgO and FeO correlating positively with CaO.

Basaltic andesite titanomagnetite and amphibole show significant inter-grain compositional variations across the respective suites of measured phenocrysts. Titanomagnetite compositions are bimodal. The first group contains variable Fe, Al and Mg contents, along with relatively low Ti concentrations (4-6 wt%), which do not vary systematically (Figure 9). Phenocrysts in the second group contain much higher Ti (8-11 wt%) and lower Mg and Al, and also show a negative correlation between Ti and Fe (Figure 9). Also, while the distinction is at the limits of analytical uncertainty, amphibole compositions appear bimodal, with one population having relatively low Fe and Si and high Al, and the other population having relatively high Fe and Si and low Al (Figure 10). Even if the bimodality is ignored as an analytical artifact, amphibole phenocrysts in the basaltic andesite vary over a much larger compositional range than amphibole from the 2008 Kasatochi andesite.

DISCUSSION

Plagioclase phenocrysts and microlites inherited from mixing end members

Microlite and Group 2 phenocryst compositions are not in equilibrium with measured groundmass glass compositions. Equilibrium Ca-Na partition coefficients between plagioclase and melt vary with magmatic H_2O content, but based on the range of these partition coefficients and measured Ca/Na molar ratios of groundmass glasses, plagioclase crystallizing from liquids equivalent in composition to groundmass glasses would have equilibrium Ca/Na molar ratios not exceeding ~3.1, even at high H_2O (Figure 11). The average microlite and Group 2 phenocryst Ca/Na ratios are ~4.8 and ~7.1,

269 respectively, with 33 of 61 measured microlites and 23 of 29 measured Group 2 rims
270 having Ca/Na ratios greater than 3.1. By contrast, the average Group 1 phenocryst Ca/Na
271 ratio is ~1.8, with only 5 of 72 measured Group 1 rims having Ca/Na ratios greater than
272 6. Group 1 phenocryst rims likely grew from a liquid similar in composition to the
273 measured groundmass glass, but most of the Group 2 rims and microlites likely grew in a
274 liquid that was significantly more mafic. The liquid that produced the Group 2
275 phenocrysts may also have had higher dissolved H_2O, but given the range of measured
276 glass Ca/Na ratios, melt H_2O concentrations would have to be unreasonably high (>8
277 wt%) to account for the full range of Group 2 phenocryst and microlite Ca/Na ratios. To
278 produce the observed compositions, the compositions of the crystallizing liquid must
279 have differed by significantly more than the observed variations in groundmass glass
280 composition.

281 The trends in bulk-rock compositions of the 2008 basaltic andesite are linear in all
282 oxides and trace elements, which could indicate pre-eruptive, two-component magma
283 mixing (Figure 2). If mixing is taken as a hypothesis for the origin of the trends in
284 basaltic andesite bulk compositions, the high-Si mixing end member would have to be a
285 medium-to-high SiO_2 basaltic andesite or low-Si andesite, similar to or more silicic than
286 the more evolved basaltic andesite samples (>55 wt% SiO_2; Figure 2), while the more
287 mafic component would need to be basaltic, similar to or more mafic than the lowest-Si
288 basaltic andesite compositions (<53 wt% SiO_2; Figure 2). These two components are
289 referred to henceforth as the silicic end member and the mafic end member, respectively.
290 The disparate plagioclase phenocryst populations further support a mixing scenario, as do
291 the compositions of the mafic minerals, which will be discussed in the next section. The

two different plagioclase populations reflect the compositional disparity between the two components in such a mixing relationship. The Group 1 phenocrysts, having grown in more silicic liquids, were inherited from the silicic end member and Group 2 phenocrysts from the more mafic end member.

The comparably high An contents of plagioclase microlites and Group 2 plagioclase phenocryst cores and rims (Figure 4) indicate that at least a large portion of plagioclase microlites in the 2008 Kasatochi basaltic andesite crystallized from the same magma as the Group 2 phenocrysts. The high FeO and MgO contents, which increase with decreasing An content of both microlites and Group 2 rims relative to Group 1 rims (Figure 7) and the disequilibrium between microlites and measured groundmass glass compositions (Figure 11) support this inference. However, a small portion of microlites contain low FeO and MgO contents even at An contents $<An_{70}$ (Figure 7). This distinction is even more obvious in the FeO/MgO ratios of plagioclase phenocryst rims and microlites, which generally decrease with An content, but also fall along two separate trends. Most Group 1 rims have higher FeO/MgO ratios than Group 2 phenocryst rims at a given An content (Figure 7).

Microlite FeO/MgO ratios generally fall to low FeO/MgO as An decreases, consistent with their formation in a similar environment to Group 2 phenocryst rims. A few microlites, however, have FeO/MgO ratios similar to or even higher than Group 1 phenocrysts (Figure 7), and they appear to create a second, high FeO/MgO trend with increasing An content. It seems most likely that Group 2 plagioclase phenocrysts and most microlites in the 2008 Kasatochi basaltic andesite were inherited from the more mafic mixing end member, while Group 1 phenocrysts and some low-An, low FeO/MgO

315 microlites were either inherited from the silicic end member or, in the case of the
316 microlites, grew from groundmass liquids during ascent.

317 It is important to note that the 2008 Kasatochi andesite was not the silicic mixing
318 end member. The mixing that formed the linear trends in basaltic andesite compositions
319 could not have involved the andesite, which lies well away from bulk compositional
320 trends defined by the basaltic andesite (e.g. Al_2O_3, P_2O_5, Y, Yb, Zn; Figure 2). Banded
321 clasts, representing mechanical mixtures of basaltic andesite and andesite, are found
322 throughout the 2008 Kasatochi deposits, but the geochemical data shown in Figure 2
323 indicates that the two were only briefly in contact. The andesite must have been staged
324 separately within the Kasatochi magmatic plumbing system from where the mixing that
325 created the basaltic andesite took place. The basaltic andesite and andesite therefore must
326 have encountered each other only during eruption. The simplest scenario for such a
327 process would have the two aforementioned mafic and silicic end members mix, with
328 insufficient time for full homogenization, and then have the new basaltic andesite mixture
329 ascend and encounter the andesite during eruption. Similar behavior has been inferred for
330 the 2006 eruption of the Augustine Island volcano in 2006, based on the compositional
331 heterogeneities andesites produced during that eruption (Larsen et al. 2010; de Angelis et
332 al. 2013). However, the possibility that the andesite ascended and encountered the
333 basaltic andesite mixture above it cannot be discounted with the current available data;
334 this question will be addressed in a subsequent study.

335 There is also evidence that the Group 1 phenocrysts have experienced episodes of
336 mixing prior to the event described here. The spikes in An content seen in Group 1
337 phenocrysts (Figure 3) are commonly associated with dissolution features, and are

interpreted as markers of periodic mafic recharge into a well-buffered silicic system. Prior studies have documented that an influx of mafic material, possibly bringing heat and increased H_2O contents, causes the outer rim of plagioclase phenocrysts to dissolve, followed by the growth of higher-An plagioclase on the outside of the dissolution surface (Tsuchiyama 1985; Davidson and Teply 1997; Clynne 1999; Tepley et al. 1999; Izbekov et al. 2004; Ruprecht and Wörner 2007). Once the system re-equilibrates, the overall normal zonation trend resumes rimward of the dissolution boundaries. Such injections may also bring in high-An plagioclase phenocrysts, which can form the high-An cores of otherwise normally zoned phenocrysts (e.g. Izbekov et al. 2004). There are also a few zones within the Group 1 phenocrysts which show an anti-correlation between Mg and An (Figure 3). This may also be related to changing Mg activity in the melt during mixing, as well as variations in Mg partitioning behavior due to compositional or kinetic effects (cf. Bottinga et al. 1966; Bindeman et al. 1998; Ginibre et al. 2002; Costa et al. 2003). More data on the internal compositional variations of the Group 1 phenocrysts is necessary to address these long-term compositional fluctuations at Kasatochi in adequate detail, but the fluctuations in An content in Group 1 phenocrysts seems to indicate that periodic mixing events do occur within the Kasatochi magma system.

Mafic phenocrysts inherited from mixing end members

The mafic phenocryst populations are not, at present suitable for thermobarometry based on mineral, mineral-liquid or mineral-mineral equilibria. In the absence of coexisting rhombohedral Fe-Ti oxides, temperatures recorded by the two

titanomagnetite compositional populations cannot be determined quantitatively. Similarly, although amphibole is abundant in the 2008 Kasatochi eruptive products, current amphibole-based thermobarometers are not applicable to the Kasatochi basaltic andesite. Models based on amphibole aluminum contents (e.g. Hammarstrom and Zen 1986; Johnson and Rutherford 1989; Anderson and Smith 1995) cannot be used, as the Kasatochi system is not saturated in quartz or biotite, as is required by such models. The plagioclase-amphibole equilibria of Holland and Blundy (1994) is potentially applicable, but Blundy and Cashman (2008) suggest that that this model does not account for non-ideal partitioning of Fe^{2+} and Mg between the amphibole M1, M2 and M3 sites. Blundy and Cashman (2008) further showed that the model systemattically underestimates T for amphiboles with high Mg#. The average amphibole Mg# at Kasatochi is 0.88, with a minimum of 0.73, indicating that application of this model to Kasatochi amphiboles is very likely to produce inaccurate results (See Figure 14b of Blundy and Cashman 2008). Also, while new models based solely on amphibole compostions continue to grow in popularity (Ridolfi et al. 2010; Ridolfi and Renzulli 2012), they are applicable only to calc-alkaline systems, and are specifically contraindicated for use in tholeiitic systems such as the 2008 Kasatochi basaltic andesite (Figure 2).

It is still possible to derive some information on mixing information from the mafic phenocryst populations within these constraints. If pre-eruptive mixing was responsible for the bulk compositional trends, high-An plagioclase microlites and the presence of two major plagioclase phenocryst populations in the basaltic andesite, it stands to reason that the compositions of the mafic phenocryst populations may also be expected to also reflect pre-eruptive mixing. In such a scenario, the overall phenocryst

population of the basaltic andesite will reflect the contribution of pre-existing mafic phenocrysts from the mafic and silicic end members (e.g., Coombs et al., 2000; Izbekov et al., 2004). The compositions of the high-Ti titanomagnetite are similar titanomagnetite compositions of the 2008 Kasatochi andesite (Figure 9), although the Mg concentrations of the andesite titanomagnetite phenpocrysts are higher. Furthmore, if the andesite was indeed colder than the basaltic andesite (Neill 2013), and compositions of the low-Al amphibole and the high-Ti magnetite compositions are similar to those of the andesite, then it seems likely that the low-Al amphibole and the high-Ti magnetite formed in a magma that was cooler, meaning that the silicic end member was cooler than the mafic end member. Also, the low-Al amphibole compositions also overlap with amphibole compositions from the andesite (Figure 10). While the incongruity of bulk chemical trends (Figure 2), and the higher Mg contents of the andesite titanomagnetite phenocrysts suggest that the andesite is not actually the silicic mixing end member, these correlations suggest that the high-Ti titanomagnetite and low-Al amphibole grew in *P*-*T*-X conditions similar to those of andesite. Such conditions would more likely be found in the silicic end member than the mafic, which would, in turn, suggest that the high-Ti titanomagnetite and low-Al amphibole would have come from the silicic end member. The 2008 Kasatochi basaltic andesite phase assemblage is therefore comprised of two separate phenocryst populations, each being contributed by their respective mixing end member.

Temperature constraints on mixing end members from plagioclase-liquid equilibria

Temperature constraints may be placed on the mixing end members using the plagioclase-liquid hygrometer/thermometer of Lange et al. (2009), which can be applied to estimate temperatures of plagioclase crystallization from a melt of know composition and dissolved H_2O concentration. Ion microprobe measurements of volatile contents in melt inclusions from 2008 Kasatochi eruptive products yield H_2O contents of ~5-7 wt% (Izbekov et al. 2009; P.E. Izbekov *unpub. data*). Group 2 phenocrysts and microlites are not in equilibrium with the groundmass glass (Figure 11), and, in the absence of constraints on the composition of liquid in equilibrium with these crystals, the Lange model cannot be applied. The Group 1 phenocrysts, however, are in equilibrium with groundmass glass compositions, and therefore the Lange et al. (2009) hygrometer can be used to determine pre-eruptive magmatic temperatures for the silicic mixing end member containing the Group 1 phenocrysts. The most primitive and most evolved measured compositions of groundmass glass are used as proxies for the most primitive and most evolved crystallizing liquid from which Group 1 plagioclase phenocrysts could reasonably be expected to grow. A comparison of natural plagioclase compositions with those predicted by the Lange et al. (2009) hygrometer reveals that the range of measured An contents of Group 1 phenocryst rims agree with predicted compositions at temperatures between 800 and 950° C (Figure 12), a plausible, if wide, range of pre-eruptive magmatic temperatures for the silicic mixing end member.

Without constraints on equilibrium liquid composition, such a method for estimating temperature for the mafic end member based on Group 2 phenocrysts is inappropriate. However, if the mafic end member was hotter than the s as the mafic phenocryst populations indicate (see Section 7.2), the lower temperature boundaries of

the mafic end member are constrained by the upper boundaries of the silicic end member to ~900° C. Furthermore, no amphibole phenocrysts from the 2008 Kasatochi basaltic andesite display reaction rims, oxidation, opacitization or any other disequilibrium textures, indicating that magmatic temperatures never exceeded those at which amphibole is stable. Therefore the upper temperature limits of amphibole stability in magmas similar to the mafic end member may be used to constrain maximum magmatic temperatures of the mafic mixing end member.

Previous experimental phase equilibria studies of Volcan Colima in Mexico and Westdahl Volcano in the central Aleutian islands, basaltic andesite systems similar to Kasatochi, suggest that amphibole would not be stable at pressures up to 200 to 300 MPa at temperatures greater than 1000° C (Moore and Carmichael 1998; Rader and Larsen 2013). Furthermore, the experiments of Gaetani et al. (1994) on basaltic andesite from the central Lau basin did not find amphibole at temperatures >1000° C at pressures up to 200 MPa, and the experiments of Pichavant et al. (2002) on basaltic andesite from Mount Pelée did not find amphibole at temperatures >1000° C at 400 MPa. Experiments on more mafic compositions produce amphibole at slightly higher temperatures, but not exceeding 1050° C at pressures up to 300 MPa (Barclay and Carmichael 2004; Nicholis and Rutherford 2004). It seems unlikely that pristine amphibole crystals such as those found in the 2008 Kasatochi basaltic andesite could exist at temperatures exceeding 1050º C, and therefore 1050° C is taken as the upper limit for plausible magmatic temperatures for the mafic end member.

Crystallization of high-An microlites due to latent heat release

Crystallization of groundmass microlites is an exothermic process which has been shown to significantly raise the temperatures of ascending magmas (e.g. Couch et al. 2003; Blundy et al. 2006; Hale et al. 2007; Pallister et al. 2008; Ruprecht and Bachmann, 2010), and as such could cause the compositions of crystallizing plagioclase to become more anorthitic, due to latent heat released during ascent-driven groundmass crystallization raising magmatic temperatures. Latent heat release must therefore be considered as a possible mechanism for the formation of high-An microlite crystallization in the 2008 Kasatochi basaltic andesite. The maximum latent heat released by plagioclase microlite crystallization can be estimated from the thermodynamic properties of the anorthite and albite end members by the relationship:

$$L = \frac{\Delta H_m}{C_p} \quad (1)$$

where ΔH_{m} is the enthalpy of melting of the plagioclase, C_p is the plagioclase heat capacity and L is change in temperature due to latent heat release (cf. Couch et al. 2003; Pallister et al. 2008).

Enthalpies of melting (ΔH_{m}) for pure albite and pure anorthite are 59280 J mol^{-1} and 81000 J mol^{-1}, respectively (Robie et al. 1978), while C_p (in J mol^{-1} K^{-1}) can be estimated for anorthite and albite as a function of temperature (T, in degrees K) using the following equations from Berman (1988):

$$C_P^{An} = 439.37 - 3734.1T^{-0.5} + (0.31702 * 10^9)T^{-3} \quad (2)$$

$$C_P^{Ab} = 393.64 - 2415.5T^{-0.5} - (7.8928 * 10^6)T^{-2} + (1.07064 * 10^9)T^{-3} \quad (3)$$

While Equation 1 provides only an estimate of the maximum temperature change due to latent heating, L can be determined as a function of plagioclase An content at different groundmass crystallinities. Depending on the amount of groundmass crystallization, the maximum change in temperature due to the formation of high-An plagioclase microlites would not exceed ~25 °C, and could be as low as ~10 °C (Figure 13), unlike in other systems where more albitic plagioclase is crystallizing and heat release is more extreme (cf. Couch et al. 2003; Pallister et al. 2008). Even a latent heat release of 25 °C would increase equilibrium An contents by only as much as ~10 mol. %, depending on T and magmatic H_2O (Figure 12), which is insufficient to cause the discrepancies in An content between the modal compositions of the microlites and Group 1 phenocrysts. Furthermore, adiabatic cooling due to degassing-driven vapor bubble expansion can also counteract the effects of latent heat release during magmatic ascent (e.g. Sparks and Pinkerton 1978; Sahagian and Proussevitch 1996; Zhang 1999; Mastin and Ghiorso 2001). To summarize, while it is significant in other volcanic systems, latent heat released by groundmass crystallization was likely negligible in the 2008 Kasatochi basaltic andesite, and was probably not a significant factor in the formation of the high-An microlites.

Decompression- and mixing-induced microlite crystallization

Decompression and degassing crystallization of an ascending magma will raise the liquidus temperature of the magma, creating effective undercooling necessary to drive crystallization (e.g. Westrich et al. 1988; Geschwind and Rutherford 1995; Hammer and

493 Rutherford 2002; Brugger and Hammer 2010). At typical magmatic ascent rates in
494 volcanic eruptions, undercoolings will be sufficiently high to induce a shift from a
495 crystallization regime dominated by growth on pre-existing phenocrysts to a regime
496 dominated by the nucleation and growth of microlites (e.g. Westrich et al. 1988;
497 Geschwind and Rutherford 1995; Hammer and Rutherford 2002; Martel and Schmidt
498 2003; McCanta et al. 2007; Brugger and Hammer 2010). In this manner, decompression
499 of the mafic end member could promote nucleation of high-An microlites from the mafic
500 end member's calcic liquids. Thus the highly calcic microlites could have originated prior
501 to the mixing process that formed the basaltic andesite, as the mafic mixing end member
502 ascended from depth.

503 Thermal differences between the two mixing end members could also cause the
504 formation of high-An microlites. When two magmas mix, the thermal contrast between
505 the two mixing end members can lead to cooling within the hotter magma, which will
506 also contribute to high effective undercoolings (e.g. Martel et al. 2006). As with
507 decompression described above, this undercooling can cause magmatic crystallization to
508 shift from a growth-dominated to a nucleation-dominated regime. This has been the basis
509 for previous models for the formation of anomalously high-An microlites in other
510 volcanic systems, with the difference in temperature between end members during
511 magma mixing responsible for the nucleation of high-An microlites in the hotter, more
512 mafic of the two end members. At Soufriere Hills, Couch et al. (2003) argue that thermal
513 convection in the magmatic storage region brought hotter, andesitic material into contact
514 with cooler, more silicic dacite, causing nucleation of microlites in the andesite. At
515 Mount Pelée, the mixing of newly injected basalt with cooler andesite caused the basalt

516 to cool and nucleate high-An microlites (Martel et al. 2006). In both cases, the microlites
517 that grew in the mafic magma were too anorthitic too be in equilibrium with the
518 groundmass melts of the hybridized magmas that were eventually erupted. A similar
519 mechanism seems likely to have operated at Kasatochi. When the hot, mafic magma
520 containing the Group 2 phenocrysts came into contact with cooler, more silicic magma
521 containing the Group 1 phenocrysts, the difference in temperature between the two would
522 have induced cooling within the mafic end member, and could have helped drive
523 nucleation of plagioclase microlites, crystallizing from the same high-Ca liquid from
524 which the Group 2 phenocrysts had previously been growing.

525 Whether the high-An microlites were formed due to decompression or mixing-
526 induced cooling, or some combination of the two, both the rapid growth of microlites and
527 the progressive assimilation of the more silicic material would act to cool the magma
528 further and drive melt evolution to less calcic compositions, as seen in the groundmass
529 glass compositions. The variations in the glass compositions are consistent with varying
530 amounts of plagioclase microlite crystallization in the groundmass (e.g. Harford et al.
531 2003; Buckley et al., 2006), without sufficient time for the compositions to homogenize
532 prior to quenching. This combination of melt evolution and silcic assimilation would, in
533 turn, trigger the formation of more albitic microlites as the liquid becomes more sodic. In
534 addition to forming new, more sodic microlites, the increasing Na activity in the melt
535 (relative to Ca) would lead to the formation of sodic rims on larger, high-An microlites
536 nucleated within the mafic end member, and the formation of more albitic rims around
537 Group 2 phenocrysts as they also came into contact with more silicic, high-Na liquids.

538 Syn-eruptive crystallization due to decompression and degassing would further promote
539 the growth of more sodic compositions (e.g. Brugger and Hammer 2010).

540

541 *Minor and trace element variations in phenocryst rims and microlites*

542 The equilibrium plagioclase-liquid partition coefficient (K_D) for Mg is not
543 strongly dependent on plagioclase compositions or magmatic intensive properties
544 (Longhi et al. 1976; Sato 1989; Phinney 1992; Bindeman et al., 1998; Aigner-Torres et
545 al. 2007), and therefore the negative relationship between An and MgO contents in
546 microlites and Group 2 phenocryst rims and the sharp increases in MgO at the rims of
547 Group 2 phenocrysts, are not a direct result of mixing-induced cooling alone. While
548 mixing between the silicic and mafic end members could increase plagioclase MgO
549 concentrations by increasing the abundance of MgO in the crystallizing liquid, it is
550 unlikely that this alone could lead to the elevated MgO concentrations seen in Kasatochi
551 microlites and Group 2 phenocryst rims. To produce the negative correlation between An
552 and MgO, the post-mixing liquid would have to be both more magnesian and less calcic,
553 a scenario inconsistent with both bulk rock and groundmass glass compositional trends
554 (Figure 2, 8).

555 A more plausible scenario can be found in the model suggested by the classic
556 paper of Bottinga et al. (1966), whereby rapid growth rates create a boundary layer of
557 melt around the crystal, which will become progressively more depleted in compatible
558 elements (such as Ca), which are taken up by the plagiclase, and enriched in incompatible
559 elements reject by the growing crystal such as Fe and Mg. As rapid, high-undercooling

crystallization progresses and the crystal grows, these boundary layers will become more and more depleted in Ca and enriched in Fe and Mg. This model has been previously invoked to explain rimward increases in FeO and MgO contents and decreases in An content in plagioclase phenocrysts from Parinacota Volcano in Chile by Ginibre et al. (2002). Similar to the scenario described at Parinacota, the inverse correlation between An content and FeO and MgO in the Group 2 phenocryst rims and microlites in the 2008 Kasatochi basaltic andesite (Figure 5, 7), as well as the zonation observed in some larger microlites (Figure 6), are probably products of this boundary layer effect, reflecting these relative changes in Ca, Fe and Mg activity in the melt boundry layers surrounding these crystals. As both high-An microlites and Group 2 phenocrysts have these rims (Figure 5, 6), it seems likely that these rims formed primarily in response to the high undercoolings created by syneruptive decompression and degassing, after the initial mixing event that led to the formation of the high-An microlites.

Unlike Mg, the K_D for Fe is expected to depend strongly on magmatic oxygen fugacity (fO_2) and temperature, which will control magmatic Fe^{2+}/Fe^{3+} speciation (Longhi et al. 1976; Sato 1989; Phinney 1992; Wilke and Behrens 1999; Sugawara 2001; Lundgaard and Tegner 2004; Aigner-Torres et al. 2007). Iron K_D's for plagioclase will increase sharply with increasing fO_2. It will, however, decrease with increasing temperature, an effect that is negligible at reducing conditions (where all available Fe is Fe^{2+}) but significant at more oxidizing conditions were Fe^{3+} is available. While dependences of Fe partitioning into plagioclase as a function of An content have been documented (Bindeman et al. 1998), such a correlation does not appear consistently in the Kasatochi basaltic andesite plagioclase. An content is dependent on temperature and

583 more strongly on p_{H2O}, the partial pressure of H_2O in the system (e.g. Lange et al. 2009).
584 Since p_{H2O} exerts a partial control on fO_2, correlated variations between plagioclase An
585 and Fe concentrations more likely result from both An content and Fe partitioning
586 changing simultaneously in response to a change in T, fO_2 and/or p_{H2O}, rather than Fe
587 partitioning changing in response to fluctuations in An content.

588 This distinction is especially germane to the Kasatochi system, in which
589 plagioclase Fe contents do not consistently depend on An content, as shown by the
590 uniformly low FeO contents of Group 1 phenocrysts cores. Even the $>An_{80}$ cores and
591 spikes in An content common in Group 1 plagioclase, are not correlated with statistically
592 significant positive or negative changes in FeO or MgO (Figure 3, 7). This suggests that
593 while previous influxes of mafic material were different enough in composition to cause
594 dissolution and re-growth on top of the dissolution surfaces, the magnitudes of these
595 forcings were insufficient to cause significant changes in Fe partitioning, or to induce the
596 rapid growth rates necessary for the formation of the boundary layers as described above.

597 Interestingly, despite microlite and Group 2 phenocryst rim FeO and MgO
598 contents increasing with decreasing An contents, FeO/MgO ratios actually *decrease*
599 slightly as microlites become more sodic (Figure 7), suggesting that the Fe K_D decreased
600 in response to either a decrease in fO_2 or an increase in temperature. An increase in
601 temperature seems unlikely, given that latent heat release is negligible (Figure 13) and
602 that the mafic end member, the source of most of the microlites and the Group 2
603 phenocrysts, would cool down, rather than heat up, during mixing. A decrease in fO_2 is
604 more realistic, and could have been induced if the silicic end member was stored under
605 more reducing conditions than the mafic. Also, Kasatochi was the largest point source

606 release of SO_2 since the 1991 eruptions of Pinatubo in the Philippines and Cerro Hudson
607 in Chile, and several studies have shown that the decompression and degassing of H_2O
608 and S-rich systems may cause decreases in fO_2 of >1 log unit due to changes in liquid-
609 vapor redox equilibria (Burgisser and Scaillet 2007; Burgisser et al. 2008).

610

611 **IMPLICATIONS**

612 Basaltic andesite from the 2008 eruption of Kasatochi Island volcano displays
613 significant heterogeneity in bulk composition, which has been interpreted as being the
614 result of magma mixing just prior to eruption. Compositions of plagioclase phenocrysts,
615 mafic phenocrysts and plagioclase microlites support this inference, suggesting that the
616 phenocryst population of the 2008 Kasatochi basaltic andesite is derived from two
617 different sources. Group 1 plagioclase phenocrysts, which are oscillatory zoned and have
618 relatively sodic rims (An_{55-65}), likely crystallized in the silicic mixing end member at
619 temperatures of 800-950 °C, along with low-Al amphibole and high-Ti titanomagnetite
620 phenocrysts. Group 2 plagioclase phenocrysts, which are dominantly >An_{80} and
621 texturally and compositionally homogenous except for abrupt shifts to more sodic
622 compositions <30 μm from their rims, likely crystallized in the mafic end member, at
623 higher temperatures (900-1000 °C), along with high-Al amphibole and low-Ti
624 titanomagnetite phenocrysts.

625 Microlites in the 2008 Kasatochi basaltic andesite are highly calcic, with
626 compositions similar to Group 2 phenocryst rims and out of equilibrium with measured
627 groundmass glass compositions. The undercooling imposed on the mafic magma due

decompression and due to contact with the cooler silicic magma likely triggered a burst of plagioclase microlite nucleation in the mafic magma, leading to the growth of high-An microlites. As the magma crystallized, and more silicic material was entrained, microlites became more sodic and thin sodic rims formed on the exteriors of Group 2 phenocrysts. The high effective undercoolings created by the mixing were exacerbated by decompression-induced degassing, causing the formation of boundary layers rich in incompatible elements (e.g., Fe, Mg) and depleted in elements which are essential plagioclase components (e.g., Ca) around microlites and Group 2 phenocrysts, leading to the formation of more sodic rims on Group 2 phenocrysts and leading to higher Fe and Mg concentrations in more sodic microlites and Group 2 rims.

ACKNOWLEDGMENTS

Grateful acknowledgments are made to C. Martel and P. Ruprecht for their insightful and constructive comments, and to T. Shea for his seemingly attentive editorial work and seemingly limitless patience. This manuscript benefited greatly from insightful discussions with W. Bohrson, C. Cameron, J. Pallister, K. Putirka, K. Severin and K. Spaleta. The authors also thank the interdisciplinary team studying ecosystem response to the eruption of Kasatochi for their assistance in the field, J. Williams and the U.S. Fish and Wildlife Service for coordinating trips to Kasatochi, and the crew of the M/V *Tiĝlax* (Captain W. Pepper, D. Erickson, E. Nelson, J. Faris, A. Velsko, J. Masui, and R. Lee) for providing safe passage to and from the island.

649 Fieldwork for this study was supported by the U.S. Fish and Wildlife Service, and
650 by the North Pacific Research Board Project #923. Analytical work was supported by
651 USGS American Recovery and Reinvestment Act (ARRA) Award #G10AC0028 to S.
652 McNutt of the University of Alaska Fairbanks, by the UAF Advanced Instrumentation
653 Laboratory, by a Jack Kleinman Grant for Volcano Research from the Community
654 Foundation of Southwest Washington, and by the United States Geological Survey
655 (USGS) Volcano Hazards Program through the Alaska Volcano Observatory, a
656 cooperative program of the University of Alaska Fairbanks, the Alaska Department of
657 Geological and Geophysical Surveys, and the USGS.

658

659 **REFERENCES**

660 Aigner-Torres, M., Blundy, J., Ulmer, P., and Pettke, T. (2007) Laser-ablation ICP-MS
661 study of trace element partitioning between plagioclase and basaltic melts: an
662 experimental approach. Contributions to Mineralogy and Petrology, 153(6), 647-
663 667. doi: 10.1007/s00410-006-0168-2

664 Anderson, J.L., and Smith, D.R. (1995) The effects of temperature and fO_2 on the al-in-
665 hornblende barometer. American Mineralogist, 80(5-6), 549-559.

666 Anderson, J.L. (1996) Status of thermobarometry in granitic batholiths. Transactions of
667 the Royal Society of Edinburgh-Earth Sciences, 87, 125-138.

668 Anderson, J.L., Barth, A.P., Wooden, J.L., and Mazdab, F. (2008) Thermometers and
669 thermobarometers in granitic systems. Reviews in Mineralogy and Geochemistry,
670 69, 121-142. doi: 10.2138/Rmg.2008.69.4

671 Arnoult, K.M., Olson, J.V., Szuberla, C.A.L., McNutt, S.R., Garces, M.A., Fee, D., and
672 Hedlin, M.A.H. (2010) Infrasound observations of the 2008 explosive eruptions
673 of Okmok and Kasatochi volcanoes, Alaska. Journal of Geophysical Research-
674 Atmospheres, 115, D00L15. doi: 10.1029/2010jd013987

675 Barclay, J., and Carmichael, I.S.E.(2004) A hornblende basalt from western Mexico:
676 Water-saturated phase relations constrain a pressure-temperature window of
677 eruptibility. Journal of Petrology, 45(3), 485-506. doi: 10.1093/Petrology/Egg091

678 Bachmann, O., and Dungan, M.A. (2002) Temperature-induced Al-zoning in hornblendes
679 of the Fish Canyon magma, Colorado. American Mineralogist, 87(8-9), 1062-
680 1076.

681 Berman, R.G. (1988) Internally-consistent thermodynamic data for minerals in the
682 system Na_2O-K_2O-CaO-MgO-FeO-Fe_2O_3-Al_2O_3-SiO_2-TiO_2-H_2O-CO_2. Journal of
683 Petrology, 29(2), 445-522. doi: 10.1093/petrology/29.2.445

684 Bindeman, I.N., Davis, A.M., and Drake, M.J. (1998) Ion microprobe study of
685 plagioclase-basalt partition experiments at natural concentration levels of trace
686 elements. Geochimica et Cosmochimica Acta, 62(7), 1175-1193.

687 Blundy, J., and Cashman, K. (2001) Ascent-driven crystallisation of dacite magmas at
688 Mount St Helens, 1980-1986. Contributions to Mineralogy and Petrology, 140(6),
689 631-650.

690 Blundy, J., and Cashman, K. (2008) Petrologic reconstruction of magmatic system
691 variables and processes. Reviews in Mineralogy and Geochemistry, 69, 179-239.
692 doi: 10.2138/Rmg.2008.69.4

693 Blundy, J., Cashman, K. and Humphreys, M. (2006) Magma heating by decompression-
694 driven crystallization beneath andesite volcanoes. Nature, 443(7107), 76-80. doi:
695 10.1038/Nature05100

696 Blundy, J.D., and Holland, T.J.B. (1990) Calcic amphibole equilibria and a new
697 amphibole-plagioclase geothermomemeter. Contributions to Mineralogy and
698 Petrology, 104(2), 208-224.

699 Bottinga Y., Kudo A., and Weill D. (1966) Some observations on oscillatory zoning and
700 crystallization of magmatic plagioclase. American Mineralogist, 51, 792-806.

701 Brugger, C.R., and Hammer, J.E. (2010) Crystallization kinetics in continuous
702 decompression experiments: implications for interpreting natural magma ascent
703 processes. Journal of Petrology, 51(9), 1941-1965. doi: 10.1093/petrology/egq044

704 Buckley, V.J.E., Sparks, R.S.J., and Wood, B. J. (2006) Hornblende dehydration
705 reactions during magma ascent at Soufrière Hills Volcano, Montserrat.
706 Contributions to Mineralogy and Petrology 151, 121–140. doi: 10.1007/s00410-
707 005-0060-5

Burgisser, A., and Scaillet, B. (2007) Redox evolution of a degassing magma rising to the surface. Nature, 445(7124), 194-197. doi: 10.1038/nature05509

Burgisser, A., Scaillet, B., and Harshvardhan (2008) Chemical patterns of erupting silicic magmas and their influence on the amount of degassing during ascent. Journal of Geophysical Research-Solid Earth, 113(B12). doi: 10.1029/2008jb005680

Clynne, M.A. (1999) A complex magma mixing origin for rocks erupted in 1915, Lassen Peak, California. Journal of Petrology, 40(1), 105-132. doi: 10.1093/petroj/40.1.105

Coats, R.R. (1956) Reconnaissance geology of some western Aleutian Islands, Alaska, Bulletin. U.S.Geological Survey Bulletin 1028-E, 83-100.

Costa, F., Chakraborty, S., and Dohmen, R. (2003) Diffusion coupling between trace and major elements and a model for calculation of magma residence times using plagioclase. Geochimica et Cosmochimica Acta, 67(12), 2189-2200

Couch, S., Harford, C.L., Sparks, R.S.J., and Carroll, M.R. (2003) Experimental constraints on the conditions of formation of highly calcic plagioclase microlites at the Soufrière Hills Volcano, Montserrat. Journal of Petrology, 44(8), 1455-1475. doi: 10.1093/petrology/44.8.1455

Davidson, J.P., and Tepley, F.J. (1997) Recharge in volcanic systems: evidence from isotope profiles of phenocrysts. Science, 275(5301), 826-829.

De Angelis, S.M.H., Larsen, J.F., and Coombs, M.L. (2013) Pre-eruptive magmatic conditions at Augustine Volcano, Alaska, 2006: evidence from amphibole geochemistry and textures. Journal of Petrology, 54(9), 1939-1961. doi:10.1093/petrology/egt037

Donovan, J.J., Kremser, D., and Fournelle, J.H. (2007) Probe for Windows User's Guide and Reference, Enterprise Edition. Probe Software Inc., Eugene, OR.

Fee, D., Steffke, A., and Garces, M. (2010) Characterization of the 2008 Kasatochi and Okmok eruptions using remote infrasound arrays. Journal of Geophysical Research-Atmospheres, 115, D00L10. doi: 10.1029/2009jd013621

Gaetani G.A., Grove T.L., and Bryan, W.B. (1994) Experimental phase relations of basaltic andesite from Hole 839B under hydrous and anhydrous conditions. In: Hawkins, J., Parson, L., Allan, J., et al. (editors) Proceedings of the Ocean Drilling Program, Scientific Results, 135, 557–563.

Geschwind, C.H., and Rutherford, M.J. (1995) Crystallization of microlites during magma ascent - the fluid-mechanics of 1980-1986 eruptions at Mount-St-Helens. Bulletin of Volcanology, 57(5), 356-370.

Gill, J.B. (1981) Orogenic andesites and plate tectonics. Springer Verlag, Berlin, Germany, 390 pp.

Ginibre, C., Wörner, G., and Kronz, A. (2002) Minor- and trace-element zoning in plagioclase: implications for magma chamber processes at Parinacota volcano,

northern Chile. Contributions to Mineralogy and Petrology, 143(3), 300-315. doi: 10.1007/s00410-002-0351-z

Hale, A.J., Wadge, G., and Mühlhaus, H.B. (2007) The influence of viscous and latent heating on crystal-rich magma flow in a conduit. Geophysical Journal International, 171(3), 1406-1429. doi: 10.1111/j.1365-246X.2007.03593.x

Hammarstrom, J.M., and Zen, E.A. (1986) Aluminum in hornblende - an empirical igneous geobarometer. American Mineralogist, 71(11-12): 1297-1313.

Hammer, J.E., Cashman, K.V., and Voight, B. (2000) Magmatic processes revealed by textural and compositional trends in Merapi dome lavas. Journal of Volcanology and Geothermal Research, 100, 165-192.

Hammer, J.E., and Rutherford, M.J. (2002) An experimental study of the kinetics of decompression-induced crystallization in silicic melt. Journal of Geophysical Research-Solid Earth, 107(B1) doi: 10.1029/2001jb000281

Harford, C.L., Sparks, R.S.J., and Fallick, A.E. (2003) Degassing at the Soufrière Hills Volcano, Montserrat, recorded in matrix glass compositions. Journal of Petrology, 44(8), 1503-1523.

Holland, T.J.B., and Blundy, J.D. (1994) Nonideal interactions in calcic amphiboles and their bearing on amphibole-plagioclase thermometry. Contributions to Mineralogy and Petrology, 116(4), 433-447.

766 Humphreys, M.C.S., Blundy, J.D., and Sparks, R.S.J. (2006) Magma evolution and open-
767 system processes at Shiveluch Volcano: Insights from phenocryst zoning. Journal
768 of Petrology, 47(12), 2303-2334. doi: 10.1093/petrology/egl045

769 Humphreys, M.C.S, Christoper, T., and Hards, V. (2009) Microlite transfer by
770 disaggregation of mafic inclusions following magma mixing at Soufrière Hills
771 Volcano, Montserrat. Contributions to Mineralogy and Petrology, 157(5), 609-
772 624.

773 Humphreys, M.C.S., Edmonds, M., Christopher, T., and Hards, V. (2010) Magma
774 hybridisation and diffusive exchange recorded in heterogeneous glasses from
775 Soufriere Hills Volcano, Montserrat. Geophysical Research Letters, 37, L00E06.

776 Izbekov, P.E., Eichelberger, J.C., and Ivanov, B.V. (2004) The 1996 eruption of
777 Karymsky volcano, Kamchatka: Historical record of basaltic replenishment of an
778 andesite reservoir. Journal of Petrology, 45(11), 2325-2345.

779 Izbekov, P., Sisson, T., Wooden, J., and Bacon, C. (2009) 2008 Kasatochi Eruption:
780 SHRIMP constraints on concentration of volatiles in melt inclusions, American
781 Geophysical Union, Fall Meeting 2009, Abstract #V51E-1775, San Francisco,
782 CA, pp. 1775.

783 Jarosewich, E. (2002) Smithsonian microbeam standards. Journal of Research of the
784 National Institute of Standards and Technology, 107, 681-685.

785 Johnson, D.M., Hooper, P.R., and Conrey, R.M. (1999) XRF Analysis of rocks and
786 minerals for major and trace elements on a single low dilution Li-tetraborate fused
787 bead. Advances in X-ray Analysis, 41, 843-867.

788 Johnson, M.C., and Rutherford, M.J. (1989) experimental calibration of the aluminum-in-
789 hornblende geobarometer with application to Long-Valley Caldera (California)
790 volcanic rocks. Geology, 17(9), 837-841.

791 Kay, S., and Kay, R. (1985) Aleutian tholeiitic and calc-alkaline magma series I: The
792 mafic phenocrysts. Contributions to Mineralogy and Petrology, 90(2), 276-290.
793 doi: 10.1007/bf00378268

794 Lange, R.A., Frey, H.M., and Hector, J. (2009) A thermodynamic model for the
795 plagioclase-liquid hygrometer/thermometer. American Mineralogist, 94(4), 494-
796 506. doi: 10.2138/am.2009.3011

797 Larsen, J.F., Nye, C.J., Coombs, M.L., Tilman, M., Izbekov, P.E., and Cameron, C.E.
798 (2010) Petrology and geochemistry of the 2006 eruption of Augustine Volcano,
799 In: Power, J.A., Coombs, M.L., and Freymueller, J.T. (editors) The 2006 eruption
800 of Augustine Volcano, Alaska, U.S. Geological Survey Professional Paper 1769,
801 15, 335-382.

802 Le Bas, M.J., Lemaitre, R.W., Streckeisen, A., and Zanettin, B. (1986) A chemical
803 classification of volcanic rocks based on the Total Alkali Silica diagram. Journal
804 of Petrology, 27(3), 745-750. doi:

Lepage, L.D. (2003) ILMAT: an Excel worksheet for ilmenite-magnetite geothermometry and geobarometry. Computers & Geosciences, 29(5), 673-678. doi: 10.1016/S0098-3004(03)00042-6

Longhi, J., Walker, D., and Hays, J.F. (1976) Fe and Mg in plagioclase. In: Proceedings of the 7th Lunar Science Conference, 1, 1281-1300.

Lundgaard, K., and Tegner, C. (2004) Partitioning of ferric and ferrous iron between plagioclase and silicate melt. Contributions to Mineralogy and Petrology, 147(4), 470-483. doi: 10.1007/s00410-004-0568-0

Martel, C. (2012) Eruption dynamics inferred from microlite crystallization experiments: application to plinian and dome-forming eruptions of Mt. Pelée (Martinique, Lesser Antilles). Journal of Petrology, 53(4), 699-725. doi: 10.1093/petrology/egr076

Martel, C., and Schmidt, B.C. (2003) Decompression experiments as an insight into ascent rates of silicic magmas. Contributions to Mineralogy and Petrology, 144(4), 397-415. doi: 10.1007/S00410-002-0404-3

Martel, C., Radadi Ali, A., Poussineau, S., Gourgaud, A., and Pichavant, M. (2006) Basalt-inherited microlites in silicic magmas: Evidence from Mount Pelée (Martinique, French West Indies). Geology, 34(11), 905-908. doi: 10.1130/g22672a.1

824 Mastin, L.G., and Ghiorso, M.S. (2001) Adiabatic temperature changes of magma-gas
825 mixtures during ascent and eruption. Contributions to Mineralogy and Petrology,
826 141(3), 307-321. doi:

827 McCanta, M.C., Rutherford, M.J., and Hammer, J.E. (2007) Pre-eruptive and syn-
828 eruptive conditions in the Black Butte, California dacite: Insight into
829 crystallization kinetics in a silicic magma system. Journal of Volcanology and
830 Geothermal Research, 160(3-4), 263-284. doi: 10.1016/J.Jvolgeores.2006.10.004

831 Miyashiro, A. (1974) Volcanic rock series in island arcs and active continental margins.
832 American Journal of Science, 274(4), 321-355. doi: 10.2475/ajs.274.4.321

833 Moore, G., and Carmichael, I.S.E. (1998) The hydrous phase equilibria (to 3 kbar) of an
834 andesite and basaltic andesite from western Mexico: constraints on water content
835 and conditions of phenocryst growth. Contributions to Mineralogy and Petrology,
836 130(3-4), 304-319.

837 Morgan, G.B., and London, D. (1996) Optimizing the electron microprobe analysis of
838 hydrous alkali aluminosilicate glasses. American Mineralogist, 81(9-10), 1176-
839 1185.

840 Neill, O.K. (2013) Petrologic and geochemical tracers of magma movement in volcanic
841 arc systems: case studies from the Aleutian Islands and Kamchatka, Russia. Ph.D.
842 Dissertation, University of Alaska Fairbanks, 207 pp.

Nicholis, M.G., and Rutherford, M.J. (2004) Experimental constraints on magma ascent rate for the Crater Flat volcanic zone hawaiite. Geology, 32(6), 489-492. doi: 10.1130/g20324.1

Nielsen, C.H., and Sigurdsson, H. (1981) Quantitative methods for electron micro-probe analysis of sodium in natural and synthetic glasses. American Mineralogist, 66(5-6), 547-552.

Pallister, J.S., Thornber, C.R., Cashman, K.V., Clynne, M.A., Lowers, H.A., Mandeville, C.W., Brownfield, I.K., and Meeker, G.P. (2008) Petrology of the 2004-2006 Mount St. Helens Lava Dome - implications for magmatic plumbing and eruption triggering. In: D.R. Sherrod, W.E. Scott and P.H. Stauffer (Editors), A Volcano Rekindled: The Renewed Eruption of Mount St. Helens, 2004-2006. U.S. Geological Survey Professional Paper 1750, pp. 647-702.

Phinney, W.C. (1992) Partition-coefficients for iron between plagioclase and basalt as a function of oxygen fugacity - implications for Archean and Lunar anorthosites. Geochimica et Cosmochimica Acta, 56(5), 1885-1895.

Pichavant, M., Martel, C., Bourdier, J.L., and Scaillet, B. (2002) Physical conditions, structure, and dynamics of a zoned magma chamber: Mount Pelee (Martinique, Lesser Antilles Arc). Journal of Geophysical Research-Solid Earth, 107(B5), doi: 10.1029/2001JB000315

Rader, E.L., and Larsen, J. F. (2013) Experimental phase relations of a low MgO Aleutian basaltic andesite at X_{H2O}= 0.7–1. Contributions to Mineralogy and Petrology, 166(6), 1593-1611.

Ridolfi, F., Renzulli, A., and Puerini, M. (2010) Stability and chemical equilibrium of amphibole in calc-alkaline magmas: an overview, new thermobarometric formulations and application to subduction-related volcanoes. Contributions to Mineralogy and Petrology, 160(1), 45-66. doi: 10.1007/S00410-009-0465-7

Ridolfi, F., and Renzulli, A. (2012) Calcic amphiboles in calc-alkaline and alkaline magmas: thermobarometric and chemometric empirical equations valid up to 1,130°C and 2.2 GPa. Contributions to Mineralogy and Petrology, 163(5), 877-895. doi: 10.1007/s00410-011-0704-6

Robie, R.A., Hemingway, B.S., and Fisher, J.R. (1978) Thermodynamic properties of minerals and related substances at 298.15 K and 1 bar (105 pascals) pressure and at higher temperatures, Bulletin. USGS Numbered Series. U.S. Geological Survey, 456 pp.

Ruprecht, P., and Bachmann, O. (2010) Pre-eruptive reheating during magma mixing at Quizapu volcano and the implications for the explosiveness of silicic arc volcanoes. Geology, 38(10): 919-922. doi: 10.1130/g31110.1

Ruprecht, P., and Wörner, G. (2007) Variable regimes in magma systems documented in plagioclase zoning patterns: El Misti stratovolcano and Andahua monogenetic

cones. Journal of Volcanology and Geothermal Research, 165(3-4), 142-162. doi: 10.1016/j.jvolgeores.2007.06.002

Sahagian, D.L., and Proussevitch, A.A. (1996) Thermal effects of magma degassing. Journal of Volcanology and Geothermal Research, 74(1-2), 19-38. doi: 10.1016/s0377-0273(96)00047-9

Sato, H. (1989) Chemistry of basalts of ODP Hole 111-504B, Supplement to: Sato, Hiroaki (1989): Mg-Fe partitioning between plagioclase and liquid in basalts of Hole 504B, ODP Leg 111: a study of melting at 1 ATM. In: Becker, K; Sakai, H; et al. (eds.), Proceedings of the Ocean Drilling Program, Scientific Results, College Station, TX (Ocean Drilling Program), 111, 17-26, doi:10.2973/odp.proc.sr.111.113.1989. PANGAEA.

Schmidt, M.W. (1992) Amphibole composition in tonalite as a function of pressure - an experimental calibration of the Al-in-hornblende barometer. Contributions to Mineralogy and Petrology, 110(2-3), 304-310.

Scott, W.E., Nye, C.J., Waythomas, C.F., and Neal, C.A. (2010) August 2008 eruption of Kasatochi Volcano, Aleutian Islands, Alaska-Resetting an island landscape. Arctic Antarctic and Alpine Research, 42(3), 250-259. doi: 10.1657/1938-4246-42.3.250

Singer, B.S., Dungan, M.A., and Layne, G.D. (1995) Textures and Sr, Ba, Mg, Fe, K and Ti compositional profiles in volcanic plagioclase: Clues to the dynamics of calc-alkaline magma chambers. American Mineralogist, 80(7-8), 776-798.

Sparks, R.S.J., and Pinkerton, H. (1978) Effect of degassing on rheology of basaltic lava. Nature, 276, 385-386.

Sugawara, T. (2001) Ferric iron partitioning between plagioclase and silicate liquid: thermodynamics and petrological applications. Contributions to Mineralogy and Petrology, 141(6), 659-686.

Tepley, F.J., Davidson, J.P., and Clynne, M.A. (1999) Magmatic interactions as recorded in plagioclase phenocrysts of Chaos Crags, Lassen Volcanic Center, California. Journal of Petrology, 40(5), 787-806. doi: 10.1093/petroj/40.5.787

Tsuchiyama, A. (1985) Dissolution kinetics of plagioclase in the melt of the system diopside-albite-anorthite, and origin of dusty plagioclase in andesites. Contributions to Mineralogy and Petrology, 89(1), 1-16. doi: 10.1007/bf01177585

Waythomas, C.F., Scott, W.E., Prejean, S.G., Schneider, D.J., Izbekov, P., and Nye, C.J. (2010a) The 7-8 August 2008 eruption of Kasatochi Volcano, central Aleutian Islands, Alaska. Journal of Geophysical Research, 115, B00B06. doi: 10.1029/2010jb007437

Waythomas, C.F., Scott, W.E., and Nye, C.J. (2010b) The geomorphology of an Aleutian volcano following a major eruption: the 7-8 August 2008 eruption of Kasatochi Volcano, Alaska, and its aftermath. Arctic Antarctic and Alpine Research, 42(3), 260-275. doi: 10.1657/1938-4246-42.3.260

Wessel, P., and Smith, W.H.F. (1996) A global self-consistent, hierarchical high-resoloution shoreline databse. Journal of Geophysical Research, 101, B4, 8741-8743.

Westrich, H.R., Stockman, H.W., and Eichelberger, J.C. (1988) Degassing of rhyolitic magma during ascent and emplacement. Journal of Geophysical Research-Solid Earth and Planets, 93(B6), 6503-6511.

Wilke, M., and Behrens, H. (1999) The dependence of the partitioning of iron and europium between plagioclase and hydrous tonalitic melt on oxygen fugacity. Contributions to Mineralogy and Petrology, 137(1-2), 102-114.

Williams, J.C., Drummond, B.A., and Buxton, R.T. (2010) Initial effects of the August 2008 volcanic eruption on breeding birds and marine mammals at Kasatochi Island, Alaska. Arctic Antarctic and Alpine Research, 42(3): 306-314. doi: 10.1657/1938-4246-42.3.306

Yogodzinski, G.M., Kay, R.W., Volynets, O.N., Koloskov, A.V., and Kay, S.M. (1995) Magnesian andesite in the western Aleutian Komandorsky region: Implications for slab melting and processes in the mantle wedge. Geological Society of America Bulletin, 107(5), 505-519. doi: 10.1130/0016 7606(1995)107<0505:maitwa>2.3.co;2

Yogodzinski, G.M., and Kelemen, P.B. (1998) Slab melting in the Aleutians: implications of an ion probe study of clinopyroxene in primitive adakite and

basalt. Earth and Planetary Science Letters, 158(1-2), 53-65. doi: 10.1016/s0012-821x(98)00041-7

Zhang, Y. (1999) Exsolution enthalpy of water from silicate liquids. Journal of Volcanology and Geothermal Research, 88(3), 201-207. doi: 10.1016/s0377-0273(98)00115-2

FIGURE CAPTIONS

Figure 1: Location map of Kasatochi Island volcano. Map created using the M_Map toolbox (R. Pawlowicz, University of British Columbia) and the GSHHG shoreline database (Wessel and Smith 1996).

Figure 2: Bulk major oxide, minor oxide and trace element vs. SiO_2 diagrams for eruptive products of the 2008 eruption of Kasatochi, showing schematic mixing relationships (double-headed arrows). Dashed fields represent hypothetical end member compositions for pre-eruptive basaltic andesite mixing trends (see text), with fields labeled "M" representing the mafic end member, and "S" representing the silicic end member. SiO_2 vs. K_2O classification diagram after Le Bas et al. (1986), with low-K/medium-K boundary from Gill (1981). SiO_2 vs. MgO/FeO classification diagram after Miyashiro (1974). Individual analyses reported in Neill (2013). Error bars indicate analytical uncertainty (2 standard deviations; R.M. Conrey, pers. comm.); in plots without error bars, analytical uncertainty is less than the size of the symbols.

963

964 Figure 3: Backscatter-electron images and core-rim compositional profiles of Group 1
965 plagioclase phenocrysts from the 2008 Kasatochi basaltic andesite. Error bars indicate
966 analytical uncertainty (2 standard deviations) calculated from repeated measurements of
967 the Lake County, Oregon, Labradorite plagioclase standard (USNM 115900; Jarosewich,
968 2002). Transects were measured using the "R2" analytical routine (see text).

969

970 Figure 4: Histogram of An contents for Group 1 and Group 2 plagioclase phenocryst
971 cores (top) and rims (middle) and plagioclase microlites (bottom) from the 2008
972 Kasatochi basaltic andesite.

973

974 Figure 5: Backscatter-electron images and core-rim compositional profiles of Group 2
975 plagioclase phenocrysts from the 2008 Kasatochi basaltic andesite. Error bars were
976 calculated in Figure 3. Transects were measured using the "R2" analytical routine (see
977 text). Dashed box in panel 5C indicates area shown in figure 6A.

978

979 Figure 6: (A) Backscatter-electron image of a Group 2 phenocryst rim (compositional
980 profile shown in Figure 5C). Low-An rim indicated by white arrows. (B) Backscatter-
981 electron image of zoned plagioclase microlites with high-An cores and lower-An rims.

982

983 Figure 7: Iron and magnesium contents, plotted as a function of An content, of Group 1
984 and Group 2 plagioclase phenocryst cores, rims and microlites from the 2008 Kasatochi
985 basaltic andesite. FeO/MgO ratios for phenocryst rims and microlites are also shown. All
986 iron reported as FeO. Error bars were calculated in Figure 3. FeO and MgO were
987 measured using the "R2" analytical routine (see text) – FeO analyses acquired using the
988 "R1" routine are not shown.

989

990 Figure 8: Compositions of groundmass glass from the 2008 Kasatochi basaltic andesite.
991 Error bars indicate analytical uncertainty (2 standard deviations) calculated from repeated
992 measurements of the VG-568 Yellowstone Rhyolite glass standard (USNM 72854;
993 Jarosewich 2002). Whole rock analyses included for comparison. Error bars refer only to
994 groundmass glass measurements; analytical uncertainty of bulk compositional analyses is
995 within the size of the symbols.

996

997 Figure 9: Compositions of titanomagnetite phenocrysts from the 2008 Kasatochi basaltic
998 andesite. Points represent the average composition of several analyses of an individual
999 phenocryst, with error bars representing the variation (2 standard deviations) of each
1000 averaged analysis. Grey field represents the range of titanomagnetite compositions from
1001 the 2008 Kasatochi andesite from Neill (2013).

1002

Figure 10: Compositions of amphibole phenocrysts from the 2008 Kasatochi basaltic andesite. Points represent the average composition of several analyses of an individual phenocryst, with error bars representing the variation (2 standard deviations) of each averaged analysis. Grey field represents the range of amphibole compositions from the 2008 Kasatochi andesite from Neill (2013).

Figure 11: Ca/Na molar ratios of Group 1 plagioclase phenocryst rims (top), Group 2 plagioclase phenocryst rims (middle) and plagioclase microlites (bottom) from the 2008 Kasatochi basaltic andesite, compared to Ca/Na of measured groundmass glass compositions. Grey fields represent measured compositions (average, ±1 standard deviation) of the given plagioclase population. Vertical dashed field represents measured groundmass glass compositions (average, ±1 standard deviation). Lines represent equilibrium plagioclase-liquid Ca/Na distribution coefficients at different magmatic H_2O concentrations (after Figure 4 of Martel et al., 2006, and references therein).

Figure 12: Natural compositions of Group 1, compared with compositions predicted by the plagioclase-liquid hygrometer of Lange et al. (2009). Compositions based on plagioclase crystallizing from liquids with compositions of the most mafic (top) and most silicic (bottom) groundmass glass composition measured in the basaltic andesite. Lines show compositions predicted by the Lange et al. (2009) hygrometer, as a function of melt H_2O content, crystallizing at temperatures indicated. Vertical grey fields represent range of natural pre-eruptive melt H_2O compositions (average, ±1 standard deviation; Izbekov

et al. 2009; P.E. Izbekov *unpub. data*). Horizontal fields represent measured An contents of Group 1 phenocrysts (average, ±1 standard deviation).

Figure 13: Predicted increases in magmatic temperature due to latent heat released by crystallization of plagioclase, as a function of the composition of the crystallizing plagioclase. See text for full description of calculations. Latent heat is calculated for a range of groundmass crystal fractions (□). Vertical grey fields represent the range of natural plagioclase microlite compositions (average, ±1 standard deviation).

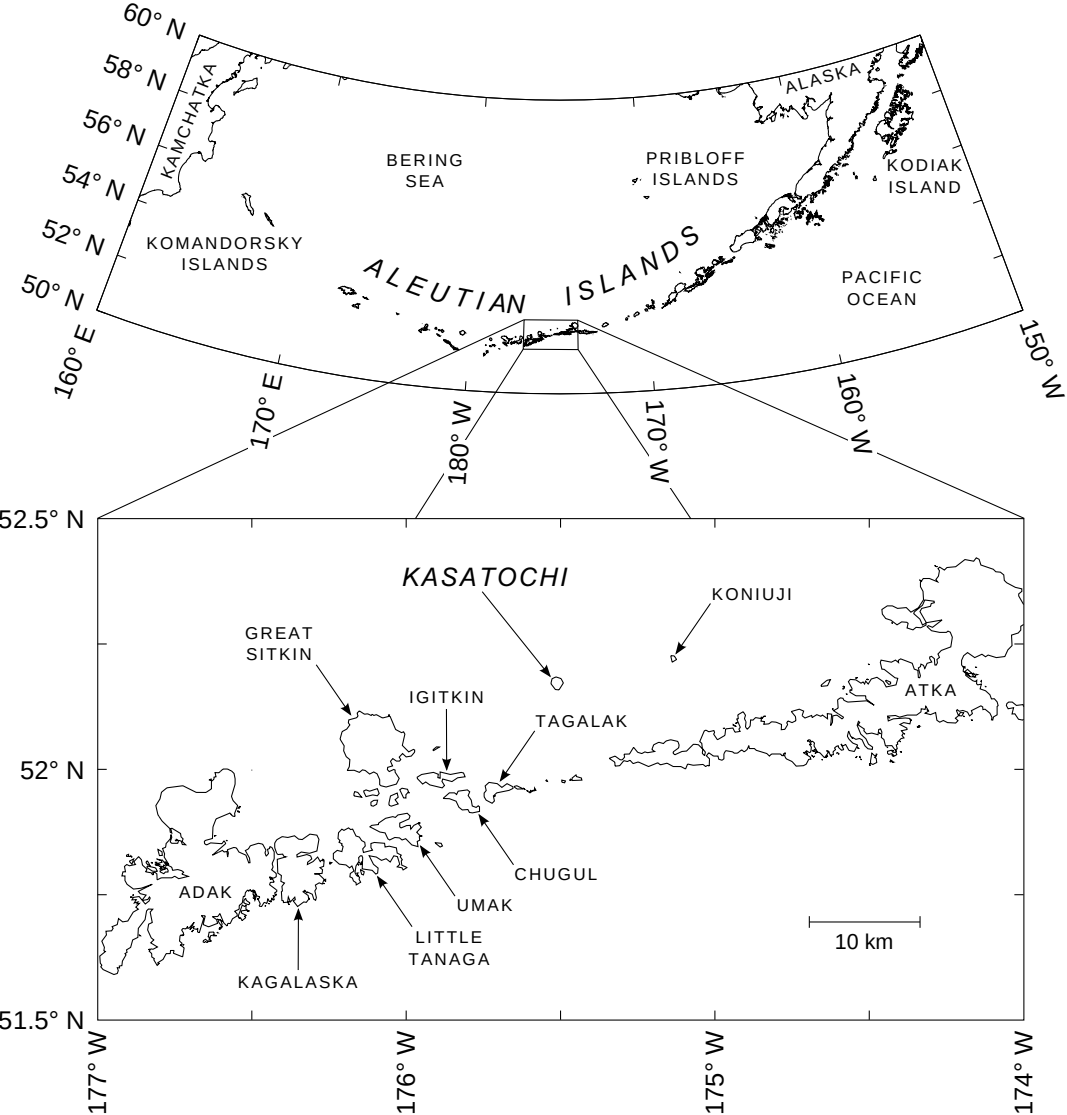
60° N
58° N
56° N
54° N
52° N
50° N
160° E
170° E
180° W
170° W
160° W
150° W
KAMCHATKA
ALASKA
BERING SEA
PRIBLOFF ISLANDS
KODIAK ISLAND
KOMANDORSKY ISLANDS
ALEUTIAN ISLANDS
PACIFIC OCEAN
52.5° N
52° N
51.5° N
177° W
176° W
175° W
174° W
KASATOCHI
KONIUJI
GREAT SITKIN
IGITKIN
TAGALAK
ATKA
CHUGUL
ADAK
UMAK
LITTLE TANAGA
KAGALASKA
10 km

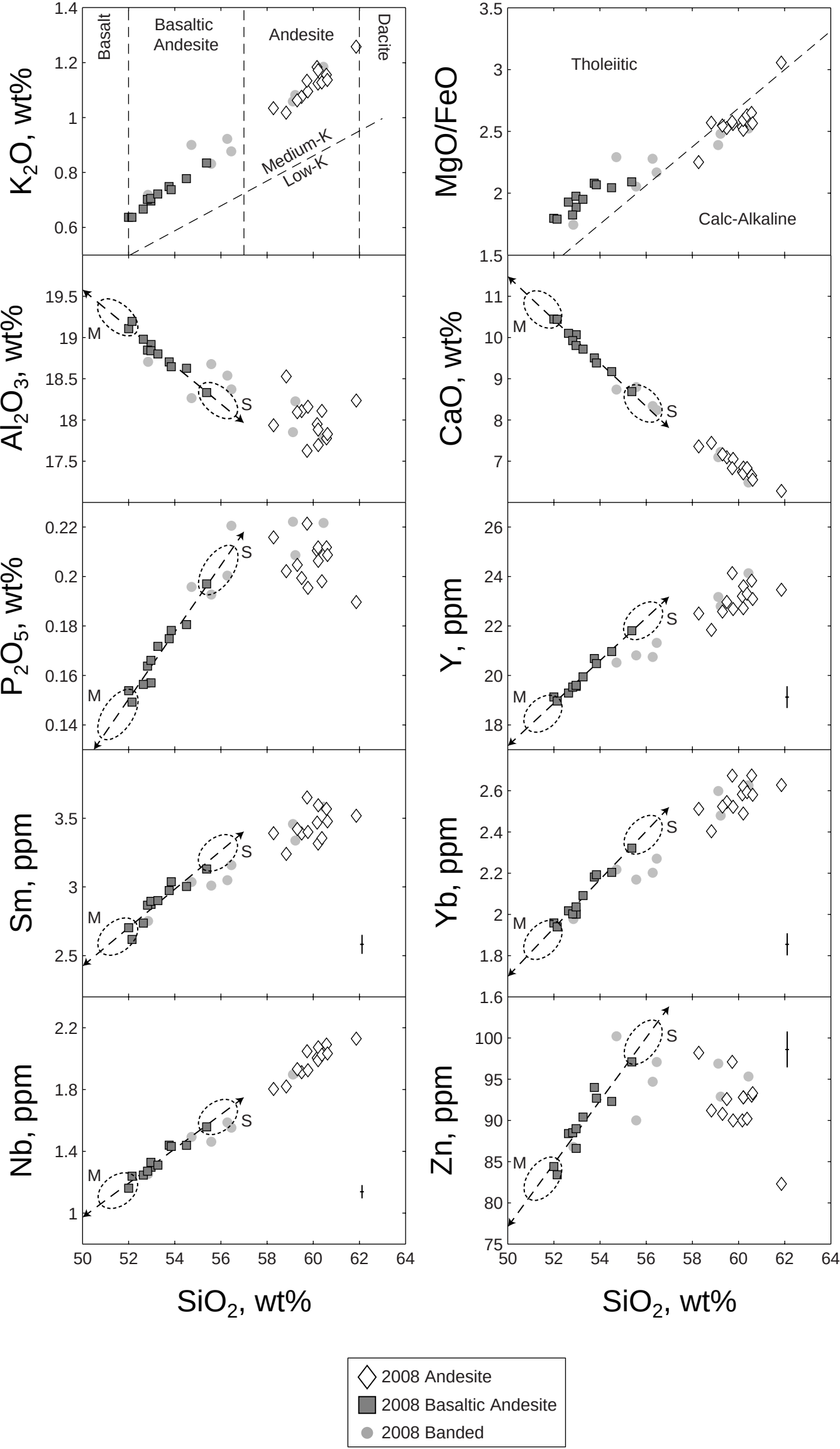
Basalt
Basaltic Andesite
Andesite
Dacite
Medium-K
Low-K
K2O, wt%
Tholeiitic
Calc-Alkaline
MgO/FeO
Al2O3, wt%
CaO, wt%
P2O5, wt%
Y, ppm
Sm, ppm
Yb, ppm
Nb, ppm
Zn, ppm
M
S
SiO2, wt%
SiO2, wt%
2008 Andesite
2008 Basaltic Andesite
2008 Banded

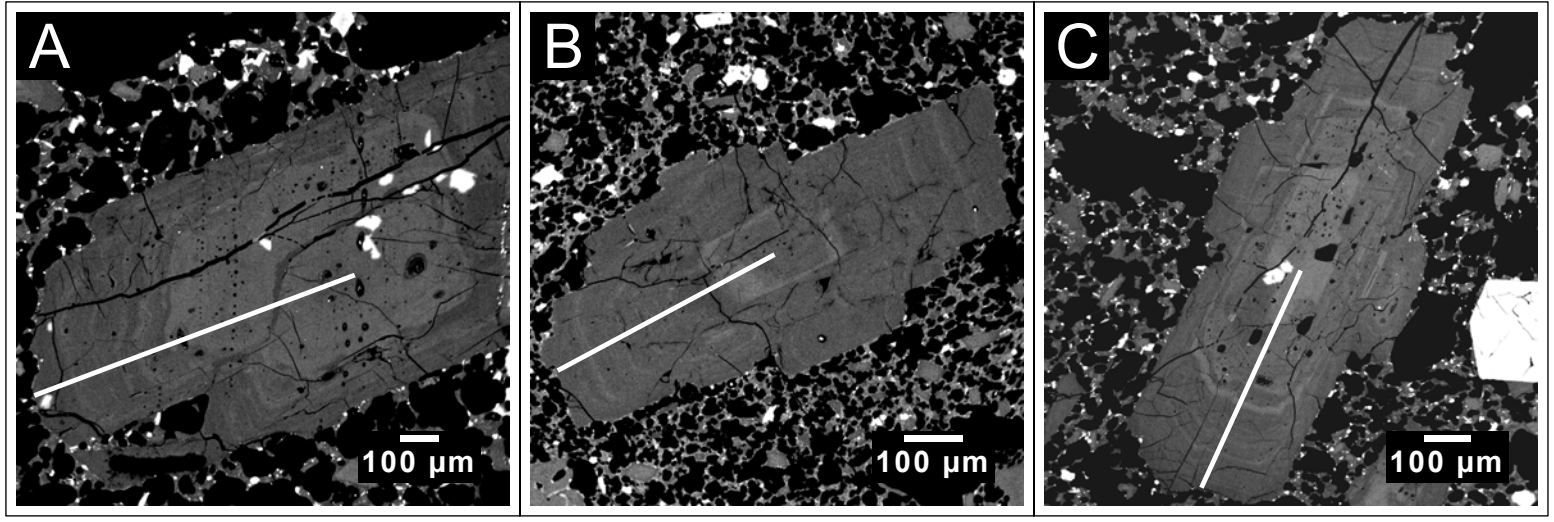
A
100 µm
B
100 µm
C
100 µm

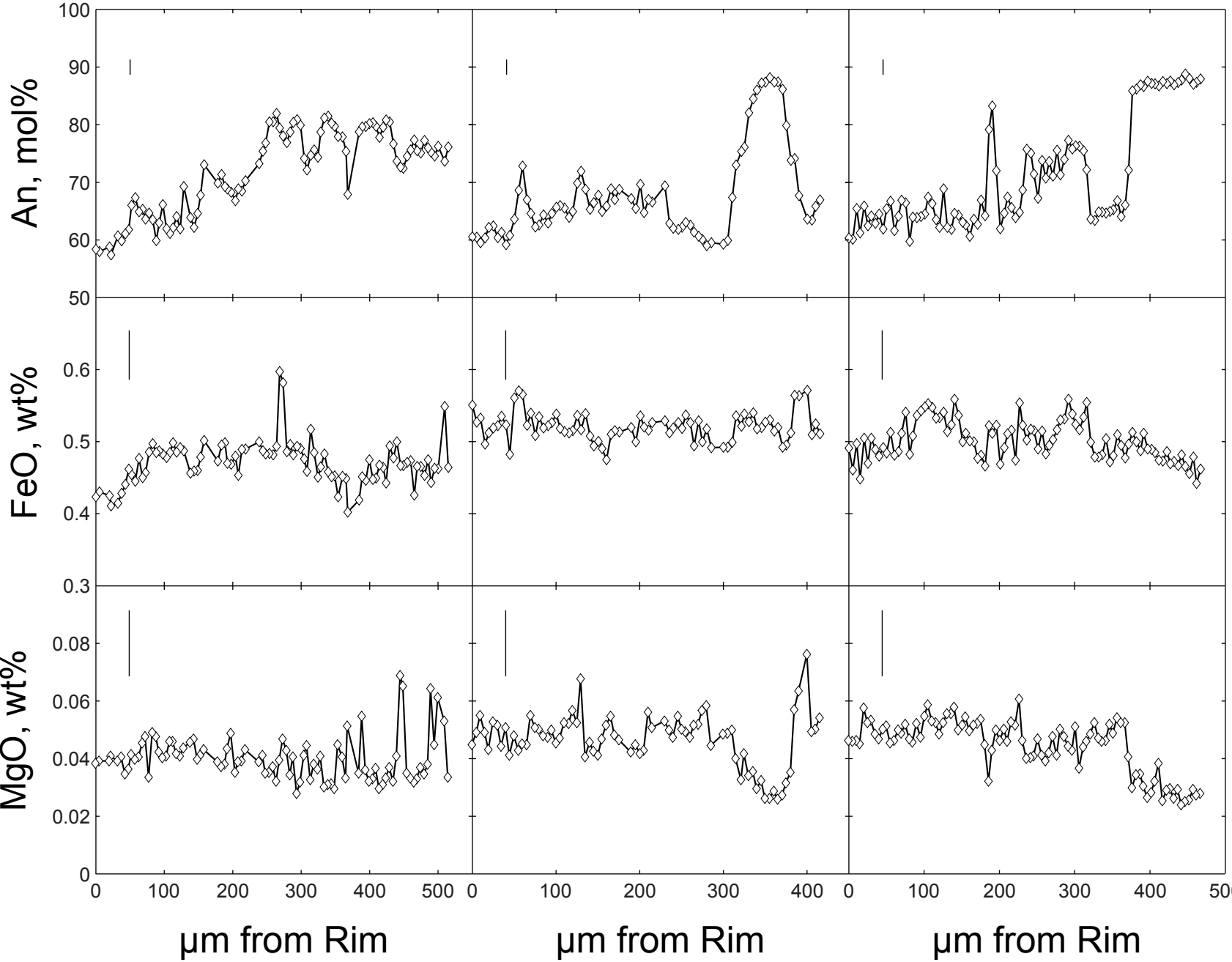
An, mol%
100
90
80
70
60
50
FeO, wt%
0.6
0.5
0.4
0.3
MgO, wt%
0.08
0.06
0.04
0.02
0
0
100
200
300
400
500
µm from Rim
µm from Rim
µm from Rim

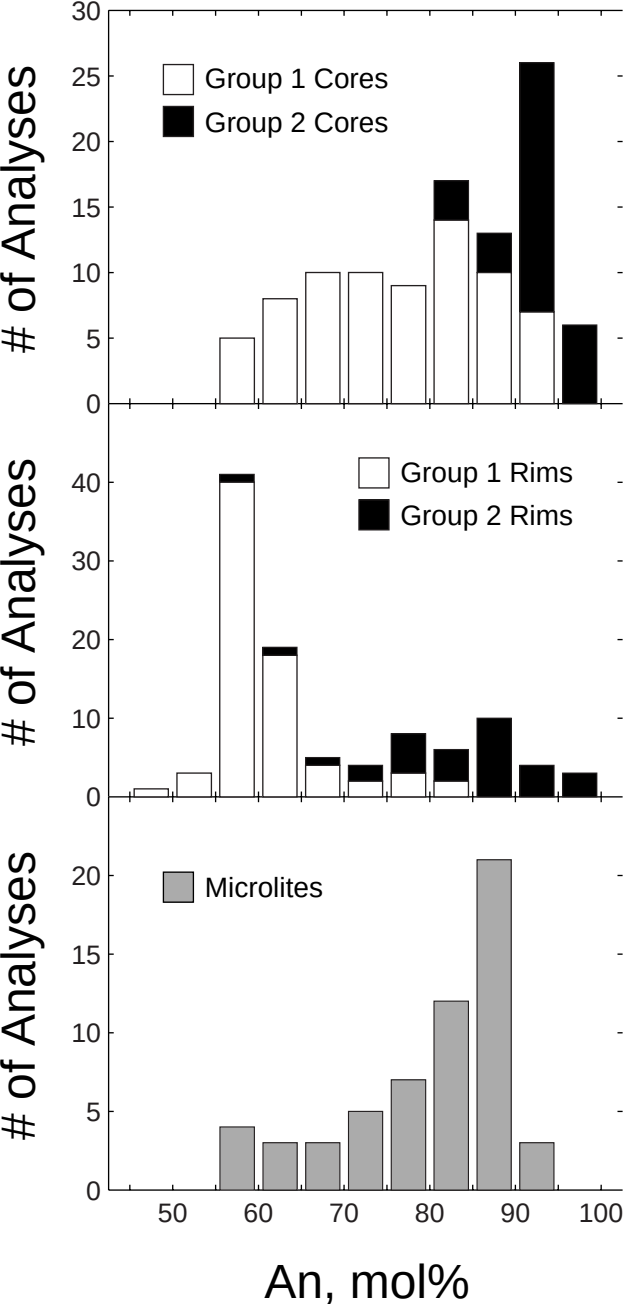
# of Analyses
Group 1 Cores
Group 2 Cores
# of Analyses
Group 1 Rims
Group 2 Rims
# of Analyses
Microlites
An, mol%

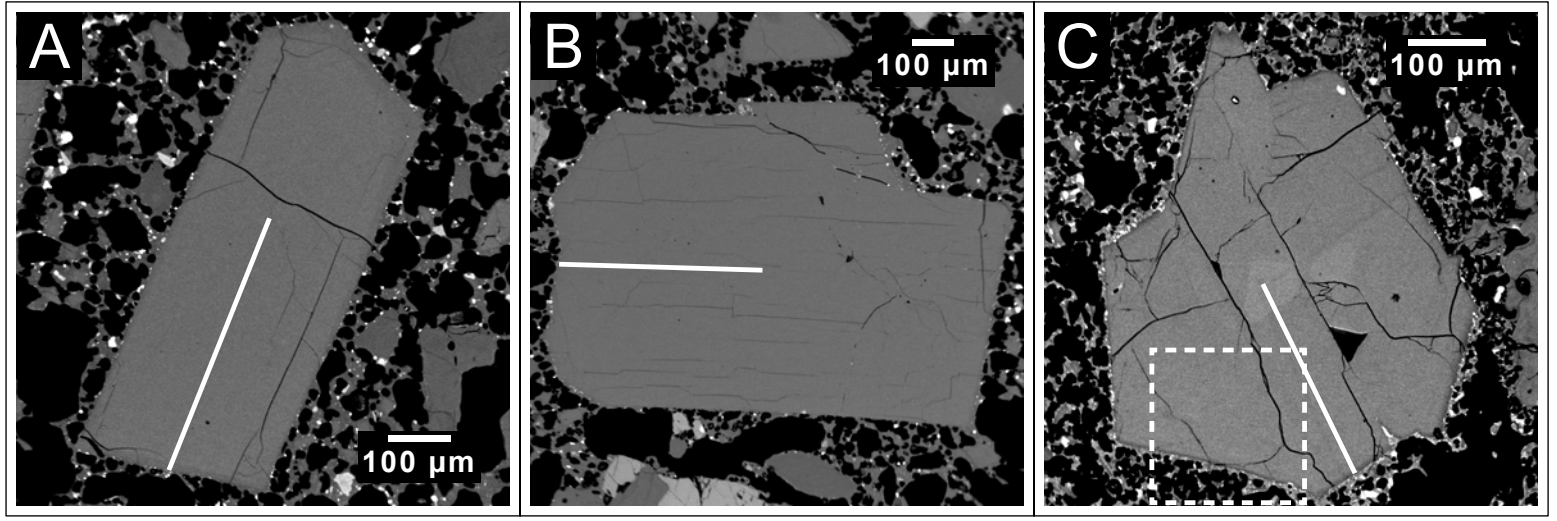
A
100 µm
B
100 µm
C
100 µm

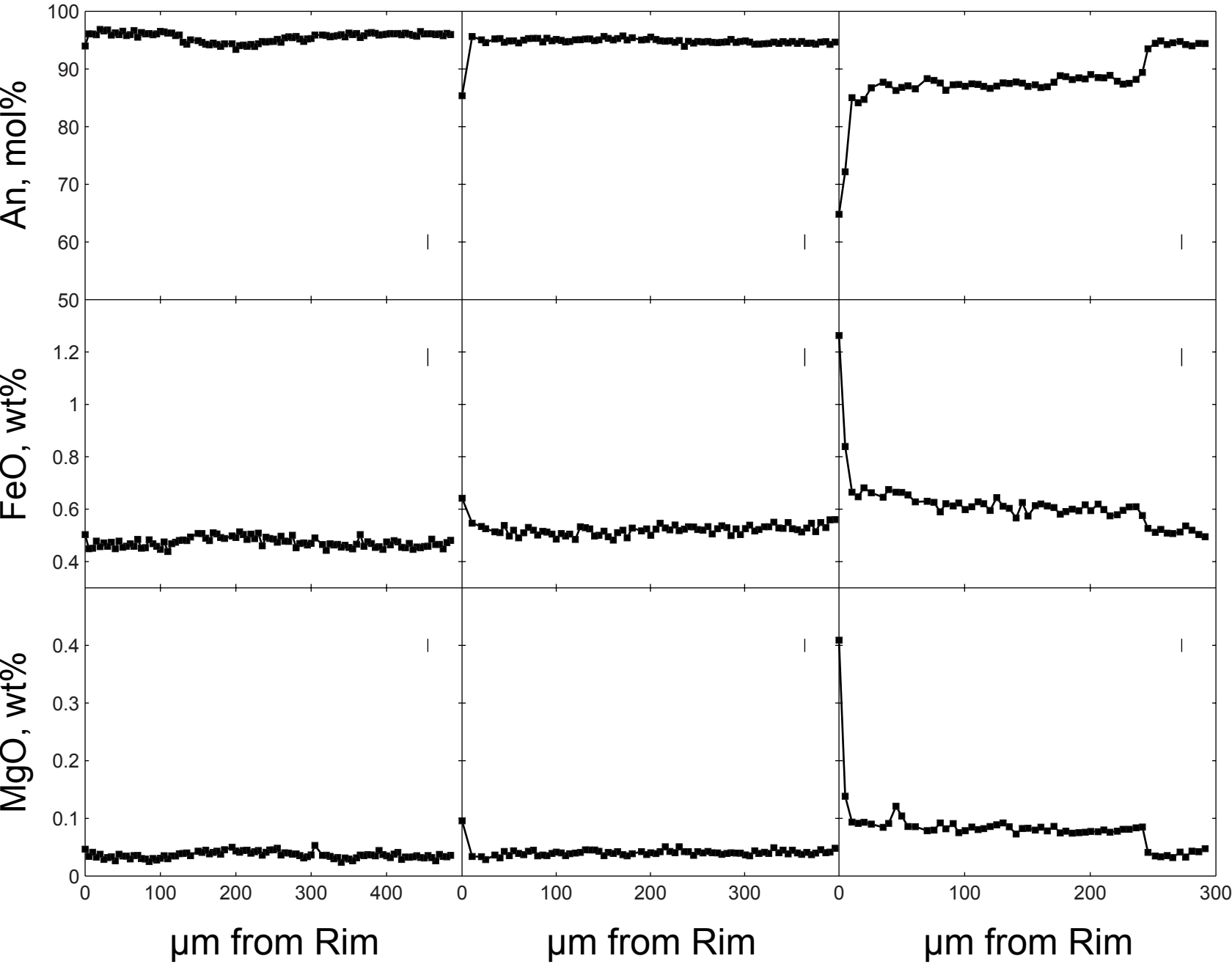
An, mol%
100
90
80
70
60
50
FeO, wt%
1.2
1
0.8
0.6
0.4
MgO, wt%
0.4
0.3
0.2
0.1
0
0
100
200
300
400
µm from Rim
0
100
200
300
µm from Rim
0
100
200
300
µm from Rim

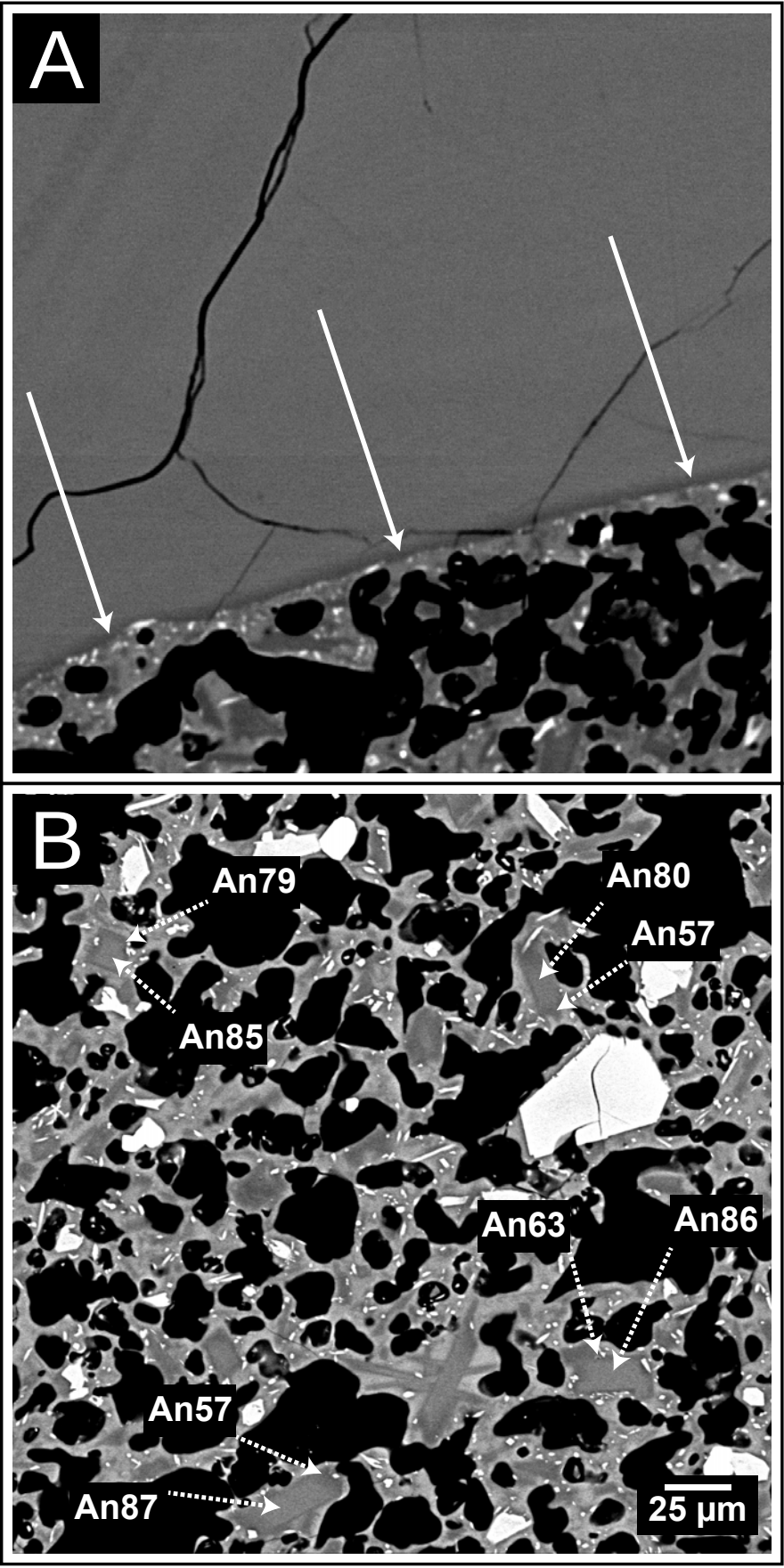
A
B
An79
An80
An57
An85
An63
An86
An57
An87
25 µm

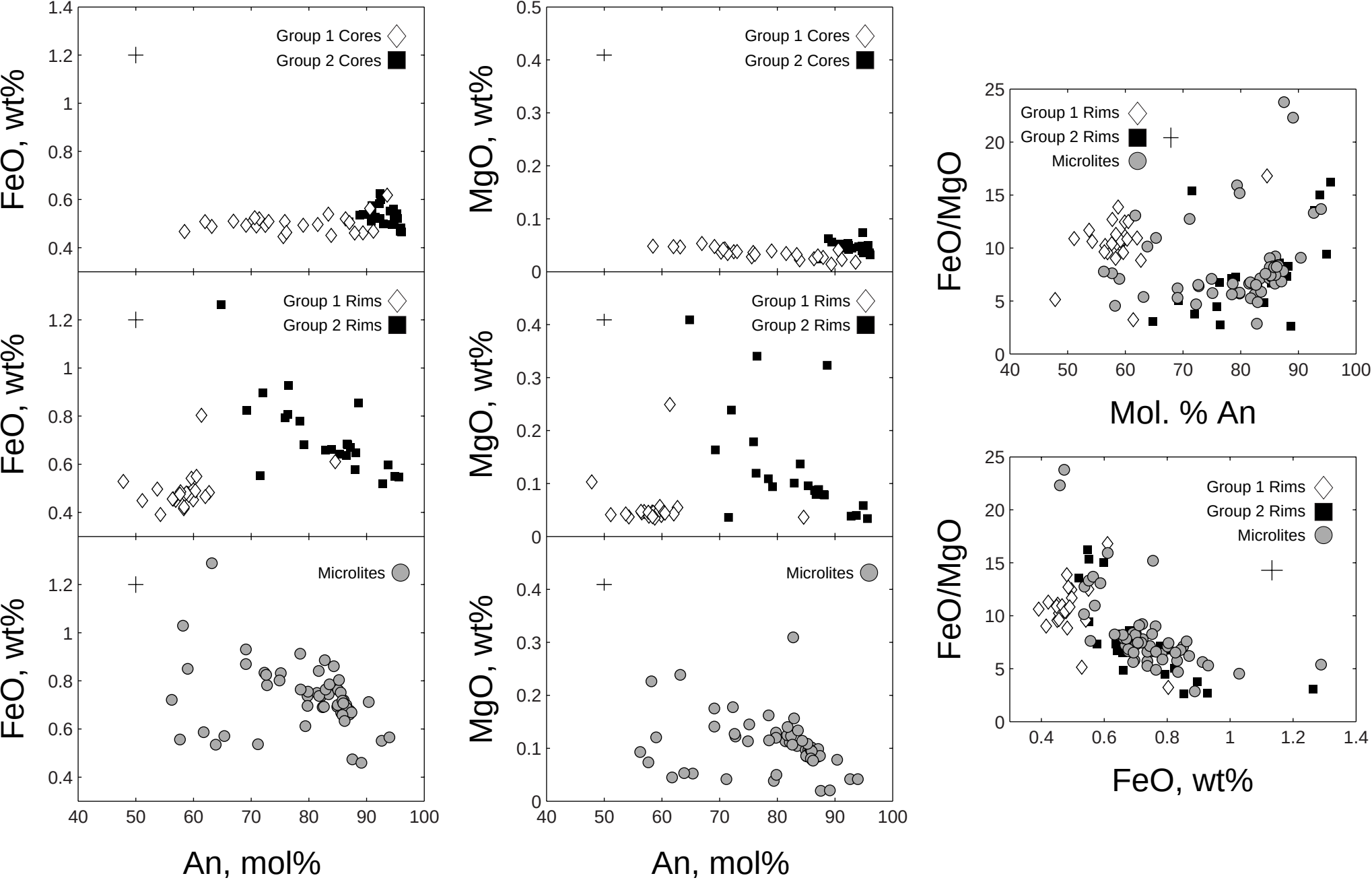
FeO, wt%
MgO, wt%
FeO/MgO
An, mol%
Mol. % An
FeO, wt%
Group 1 Cores
Group 2 Cores
Group 1 Rims
Group 2 Rims
Microlites

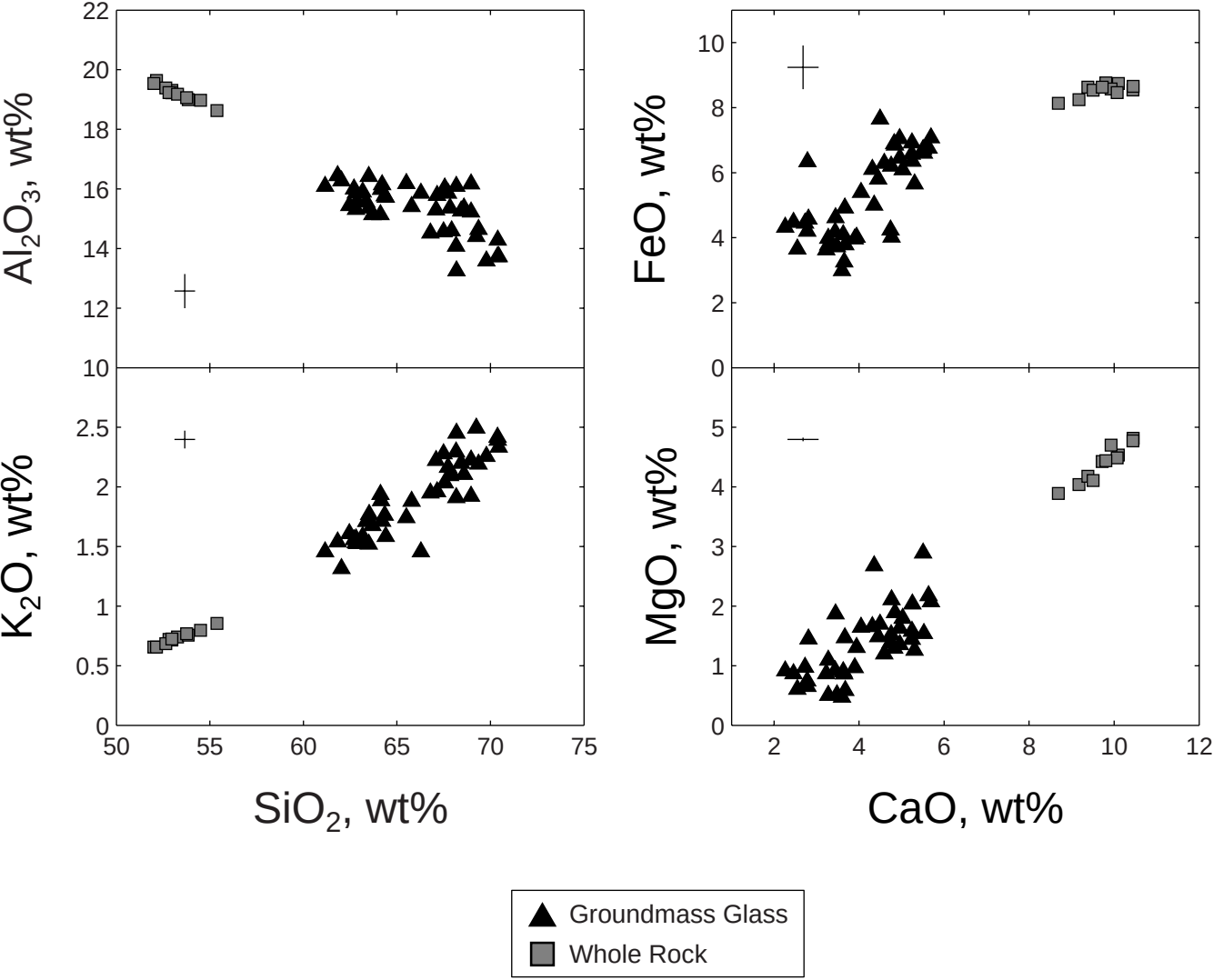
Al_2O_3, wt%
FeO, wt%
K_2O, wt%
MgO, wt%
SiO_2, wt%
CaO, wt%
Groundmass Glass
Whole Rock

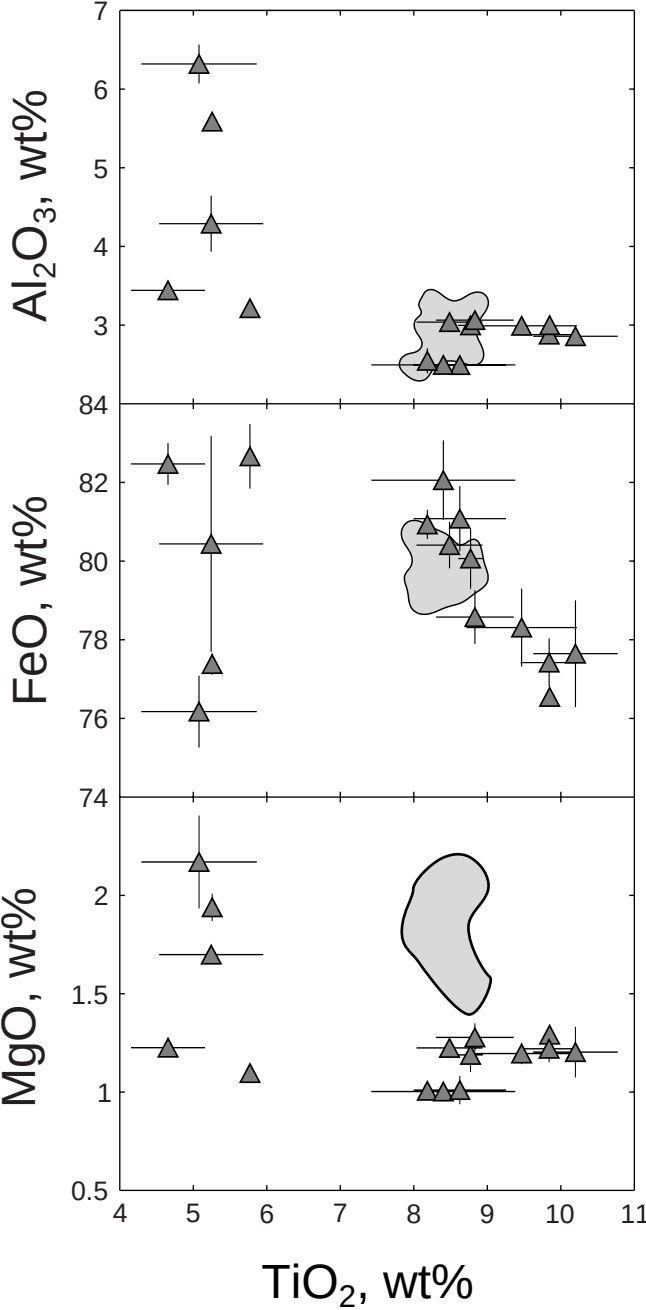
Al2O3, wt%
FeO, wt%
MgO, wt%
TiO2, wt%
7
6
5
4
3
84
82
80
78
76
74
2
1.5
1
0.5
4
5
6
7
8
9
10
11

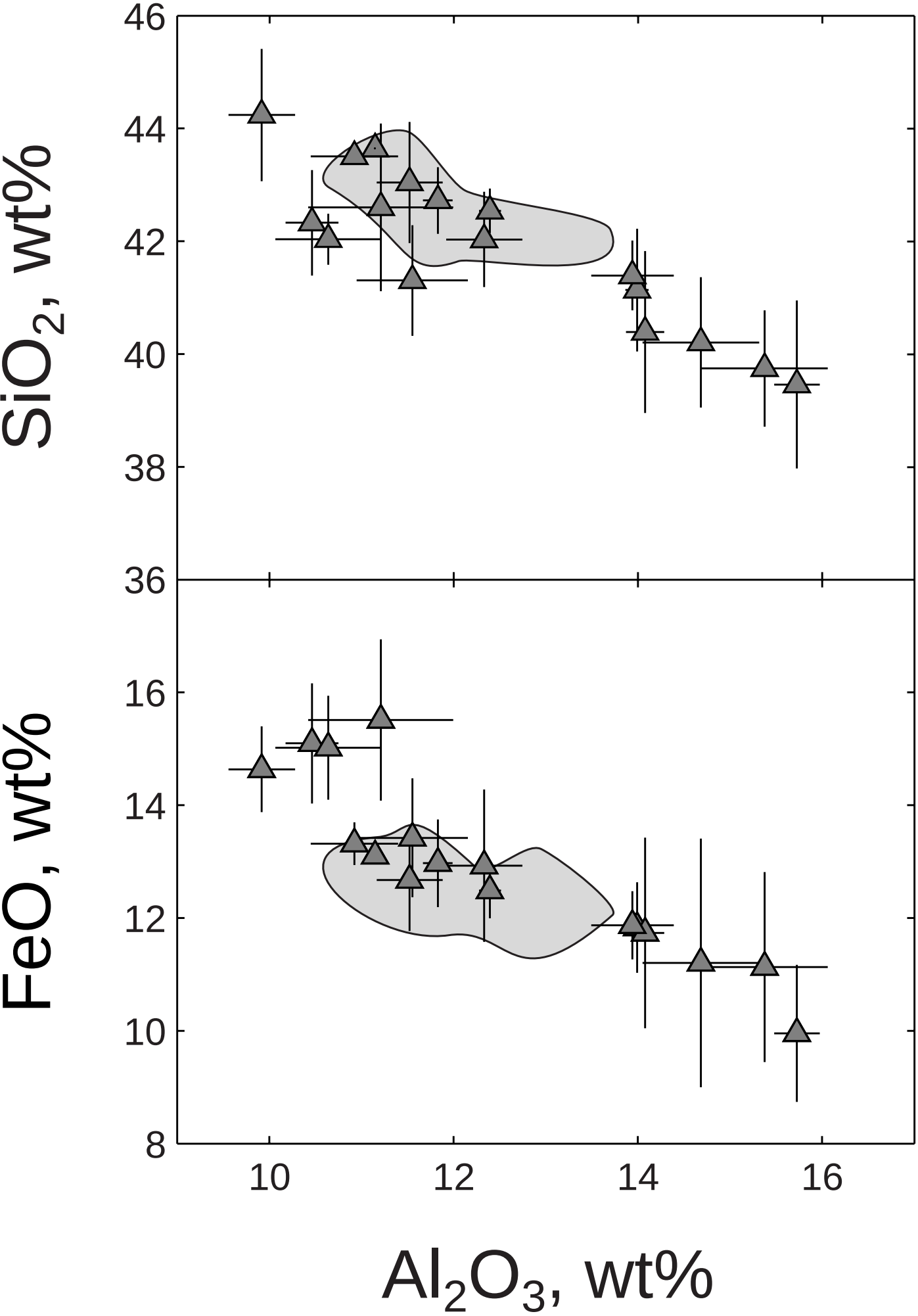
46
44
42
40
38
36
SiO2, wt%
16
14
12
10
8
FeO, wt%
10
12
14
16
Al2O3, wt%

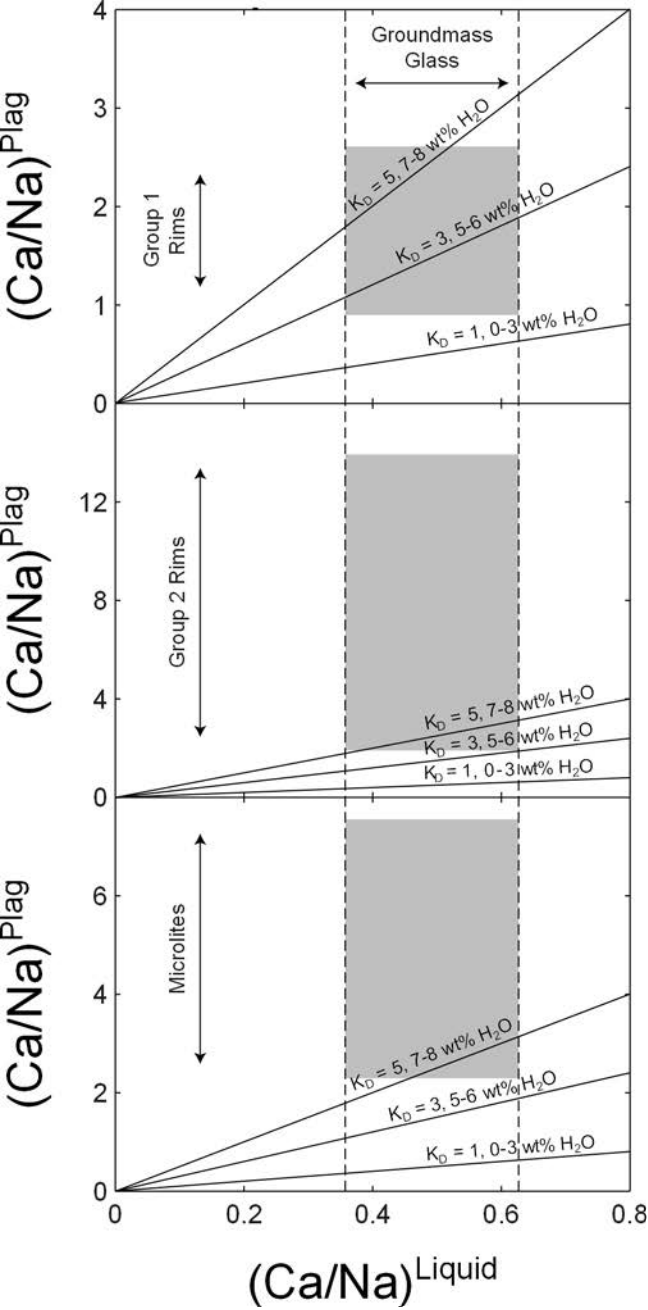
Groundmass Glass
Group 1 Rims
K_D = 5, 7-8 wt% H_2O
K_D = 3, 5-6 wt% H_2O
K_D = 1, 0-3 wt% H_2O
Group 2 Rims
K_D = 5, 7-8 wt% H_2O
K_D = 3, 5-6 wt% H_2O
K_D = 1, 0-3 wt% H_2O
Microlites
K_D = 5, 7-8 wt% H_2O
K_D = 3, 5-6 wt% H_2O
K_D = 1, 0-3 wt% H_2O
$(Ca/Na)^{Plag}$
$(Ca/Na)^{Liquid}$
0
0.2
0.4
0.6
0.8
1
2
3
4
6
8
12

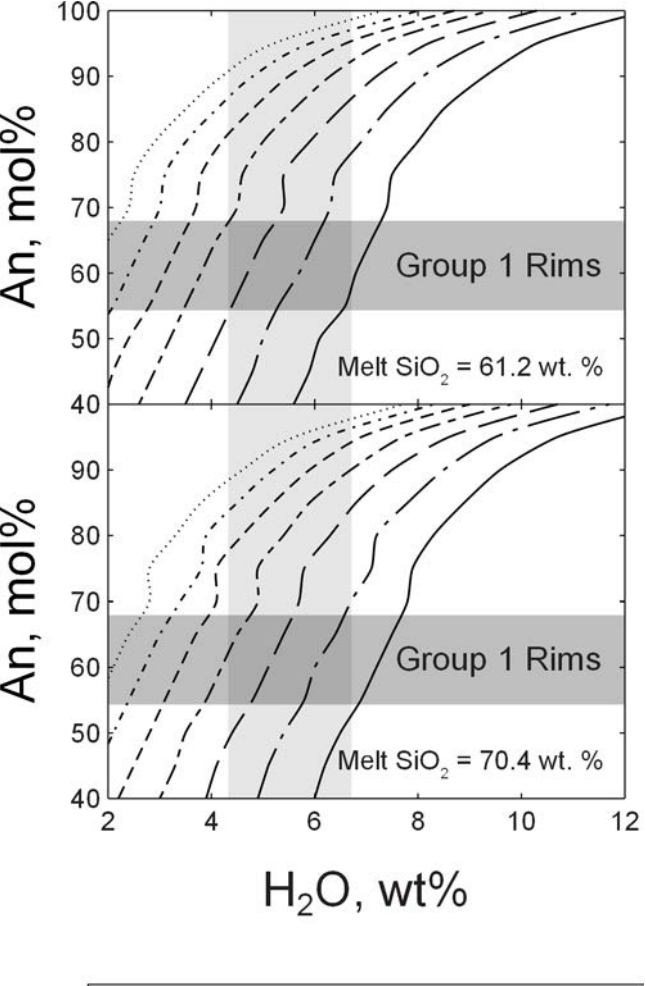
An, mol%
100
90
80
70
60
50
40
Group 1 Rims
Melt SiO2 = 61.2 wt. %
An, mol%
Group 1 Rims
Melt SiO2 = 70.4 wt. %
2
4
6
8
10
12
H2O, wt%

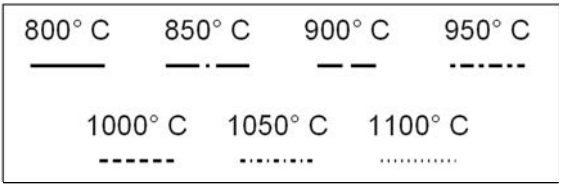
800° C
850° C
900° C
950° C
1000° C
1050° C
1100° C

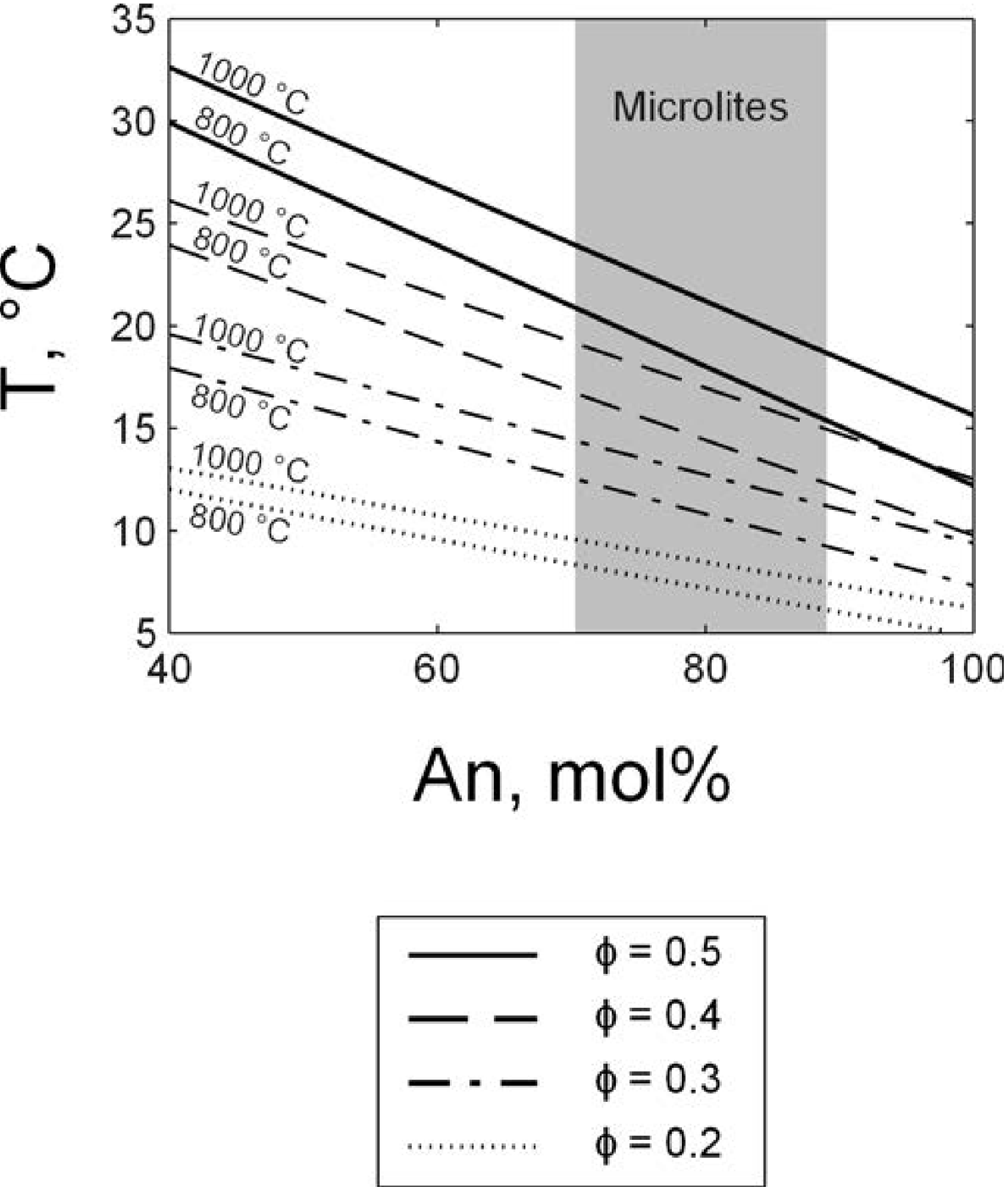
T, °C
35
30
25
20
15
10
5
40
60
80
100
An, mol%
Microlites
1000 °C
800 °C
1000 °C
800 °C
1000 °C
800 °C
1000 °C
800 °C
ϕ = 0.5
ϕ = 0.4
ϕ = 0.3
ϕ = 0.2